Kidney International (2015.2) 87(2):370-381.

Endothelin-1, but not angiotensin II, induces afferent arteriolar myosin diphosphorylation as a potential contributor to prolonged vasoconstriction

Kosuke Takeya, Xuemei Wang, Iris Kathol, Kathy Loutzenhiser, Rodger Loutzenhiser, Michael P. Walsh

TITLE PAGE – word count:3682.

Endothelin-1, but not angiotensin II, induces afferent arteriolar myosin diphosphorylation

Kosuke Takeya,[1,2,3] Xuemei Wang,[2] Iris Kathol,[1,2] Kathy Loutzenhiser,[2] Rodger Loutzenhiser,[2] and Michael P. Walsh[1]

Smooth Muscle Research Group and Departments of [1]Biochemistry and Molecular Biology and [2]Physiology and Pharmacology, Faculty of Medicine, University of Calgary, 3330 Hospital Drive N.W., Calgary, Alberta T2N 4N1, Canada

[3]Present address: Department of Physiology, Asahikawa Medical College, Midorigaoka-Higashi 2-1-1-1, Asahikawa 078-8510, Hokkaido, Japan

Correspondence: Michael P. Walsh, Department of Biochemistry and Molecular Biology, Faculty of Medicine, University of Calgary, 3330 Hospital Drive N.W., Calgary, Alberta T2N 4N1, Canada. Tel: 403-220-3021; Fax: 403-270-2211; E-mail: walsh@ucalgary.ca

Acknowledgements: This work was supported by a grant (MOP-93806) to R.L. and M.P.W. from the Canadian Institutes of Health Research. R.L. is an Alberta Innovates - Health Solutions (AI-HS) Scientist. M.P.W. is an AI-HS Scientist and Canada Research Chair (Tier 1) in Vascular Smooth Muscle Research.

Running headline: Myosin diphosphorylation in the afferent arteriole

ABSTRACT

Bolus administration of endothelin-1 (ET-1) elicits long-lasting renal afferent arteriolar vasoconstriction, in contrast to transient constriction induced by angiotensin II (Ang II). Vasoconstriction is generally evoked by myosin regulatory light chain (LC_{20}) phosphorylation at Ser19 by myosin light chain kinase (MLCK), which is enhanced by Rho-associated kinase (ROCK)-mediated inhibition of myosin light chain phosphatase (MLCP). LC_{20} can be diphosphorylated at Ser19 and Thr18, resulting in reduced rates of dephosphorylation and relaxation. We tested the hypothesis that LC_{20} diphosphorylation contributes to sustained ET-1-, but not transient Ang II-induced vasoconstriction. ET-1 treatment of isolated arterioles elicited a concentration- and time-dependent increase in LC_{20} diphosphorylation at Thr18 and Ser19. Inhibition of MLCK or ROCK reduced ET-1-evoked LC_{20} mono- and diphosphorylation. Pre-treatment with an ET_B receptor antagonist, but not an ET_A receptor antagonist, abolished LC_{20} diphosphorylation, and an ET_B receptor agonist induced LC_{20} diphosphorylation. In contrast, Ang II elicited phosphorylation exclusively at Ser19. We conclude that ET-1 and Ang II induce afferent arteriolar constriction via LC_{20} phosphorylation at Ser19 due to Ca^{2+} activation of MLCK and ROCK-mediated inhibition of MLCP, and ET-1, but not Ang II, induces phosphorylation of LC_{20} at Thr18, which could contribute to the prolonged vasoconstrictor response to ET-1.

KEYWORDS: endothelin-1; angiotensin II; afferent arteriole; myosin regulatory light chain; diphosphorylation; Rho-associated kinase

INTRODUCTION

Endothelin-1 (ET-1), a potent peripheral vasoconstrictor, is implicated in several renal disorders.[1-3] The ability of ET-1 to reduce renal blood flow resembles that of angiotensin II (Ang II), a renal-selective vasoconstrictor.[4] However, whereas Ang II contributes to renal vascular tone in physiologic settings, and to normal regulation of renal hemodynamics,[5] ET-1-dependent renal vasoconstriction is seen only in pathologic settings associated with abnormal renal vascular function and reduced glomerular filtration.[1-3,6-8] Thus, while both ET-1 and Ang II are potent renal vasoconstrictors, the nature of renal vascular tone induced by these two peptides is qualitatively distinct. This study addresses the biochemical determinants underlying these differences, focusing on the unique actions of ET-1 on the afferent arteriole.

The renal afferent arteriole conducts blood flow to the glomerular capillaries where the blood is filtered prior to its return to the general circulation via the efferent arterioles. ET-1 effects are mediated by G protein-coupled ET_A and ET_B receptors; both are detected in renal vascular smooth muscle[9] and both are involved in renal vasoconstriction.[10-13] ET_B receptors, however, are also expressed on endothelial cells and mediate NO-dependent relaxation.[13,14] One of the most striking differences in the nature of the Ang II-induced renal vasoconstriction compared to that induced by ET-1 is the duration of the response. When administered as a bolus, Ang II (via the AT_1 receptor) produces a transient

vasoconstriction, whereas brief exposure to ET-1 results in a sustained increase in renal vascular resistance.[4] Indeed, ET-1 was first reported as a long-acting vasoconstrictor both *in vitro* and *in vivo*.[15]

The key event in the activation of vascular smooth muscle contraction is the Ca^{2+}-dependent phosphorylation at Ser19 of the two 20-kDa regulatory light chain subunits (LC_{20}) of smooth muscle myosin II by calmodulin-dependent myosin light chain kinase (MLCK).[16] Contractile stimuli often also elicit Ca^{2+} sensitization, an increase in force without a change in cytosolic free Ca^{2+} concentration ($[Ca^{2+}]_i$), which is commonly achieved by activation of the small GTPase RhoA and its downstream target Rho-associated kinase (ROCK), leading to inhibition of myosin light chain phosphatase (MLCP) and increased LC_{20} phosphorylation.[17] Whereas MLCK phosphorylates LC_{20} exclusively at Ser19 *in situ*,[18] integrin-linked kinase (ILK)[19] and zipper-interacting protein kinase (ZIPK)[20] phosphorylate LC_{20} at Ser19 and Thr18, both in a Ca^{2+}-independent manner. Recently, we demonstrated, in rat caudal arterial smooth muscle strips, that: (i) Ser19 phosphorylation accounts for the level of steady-state force attained in response to contractile stimuli, and (ii) additional phosphorylation at Thr18 slows the rates of LC_{20} dephosphorylation and relaxation.[18]

An important limiting factor in studies of the molecular mechanisms and signal transduction pathways involved in the regulation of afferent arteriolar contractility is the tiny size of the vessels, making biochemical analysis challenging. A single afferent arteriole (~18 μm in diameter) is

approximately one-tenth the size of a human eyelash, and contains <100 smooth muscle cells and ~50 pg (2.5 fmol) of LC_{20}.[21] We have addressed this problem by developing and refining highly sensitive techniques for the detection and quantification of proteins and protein phosphorylation. By introducing a streptavidin-biotin amplification step in the western blot procedure, we identified the smooth muscle myosin heavy chain isoforms that are expressed in the afferent and efferent arteriole.[22] Capillary isoelectric focusing to separate phosphorylated and unphosphorylated LC_{20}, coupled with laser-induced fluorescence detection following fluorescent labeling of LC_{20}, provided >3,000-fold enhanced sensitivity over existing methods.[23] The latter technique, however, proved tedious and time consuming, which led us to adapt the Phos-tag SDS-PAGE technique[24] to quantify LC_{20} phosphorylation.[21] In this simple gel electrophoretic technique, a phosphate-binding ligand is covalently bound to acrylamide during polymerization of a Laemmli SDS gel. In the presence of Mn^{2+} ions, phosphoproteins bind to the ligand, which retards their movement through the gel relative to their unphosphorylated counterparts. By combining this technique with more efficient extraction of tissue proteins at increased SDS concentration, fixation of the transblotted protein on polyvinylidene difluoride membrane, introduction of a streptavidin-biotin amplification step, and enhanced chemiluminescence detection using an antibody that recognizes all forms of LC_{20} (phosphorylated and unphosphorylated), we were able to quantify LC_{20} phosphorylation in three pooled afferent arterioles.[21]

In the current study, we exploited this technique to compare the molecular mechanisms underlying the distinct vasoconstrictor responses of the renal afferent arteriole to ET-1 and Ang II, and further increased the sensitivity of LC_{20} detection and quantification so that LC_{20} phosphorylation can be quantified reliably with a single afferent arteriole. Specifically, we tested the hypothesis that the molecular basis of the different contractile responses of the afferent arteriole to ET-1 and Ang II (sustained *versus* transient vasoconstriction) involves LC_{20} diphosphorylation in the case of ET-1 and monophosphorylation in the case of Ang II.

RESULTS

ET-1- and Ang II-induced afferent arteriolar vasoconstriction

We demonstrated previously that equal concentrations of ET-1 and Ang II elicit similar decrements in renal perfusion.[4] In the present study, 0.1 nmol/L ET-1 and Ang II reduced afferent arteriolar diameters from 19.0 ± 0.6 to 9.1 ± 0.5 μm (n = 8) and from 17.7 ± 0.5 to 5.4 ± 0.6 μm (n = 5), respectively (Supplemental Table S1), i.e. similar reductions in arteriolar diameter were observed with the two agonists. Kinetic analysis of these vasoconstrictor responses revealed that the Ang II-induced constriction was significantly faster than the ET-1-induced response (Figure 1). Vasodilation following washout of ET-1 was also much slower than following washout of Ang II (Figure 2).

ET-1-induced vasoconstriction, increased $[Ca^{2+}]_i$ and the effect of diltiazem

ET-1-induced vasoconstriction of the afferent arteriole *in situ* was partially reversed by inhibition of voltage-gated Ca^{2+} channels with diltiazem in a concentration-dependent manner (Figure 3A and B). On the other hand, ET-1 elicited a sustained increase in $[Ca^{2+}]_i$ in isolated afferent arterioles, which was largely reversed by diltiazem (Figure 3C and D). Quantitative comparison of the effects of 1 and 10 μmol/L diltiazem on ET-1-induced vasoconstriction and $[Ca^{2+}]_i$ demonstrated that marked inhibition of Ca^{2+} entry via voltage-gated Ca^{2+} channels had modest impact on arterial diameter (Figure 3E),

suggesting that the sustained vasoconstrictor response to ET-1 is not due entirely to sustained Ca^{2+} entry and maintenance of a high level of activation of MLCK. The reason for using different concentrations of ET-1 in the *in situ* hydronephrotic kidney preparation (0.1 nmol/L) compared to isolated afferent arterioles (10 nmol/L) lies in the fact that the membrane potential in *in situ* perfused afferent arterioles pressurized to 80 mm Hg lies near the threshold activation potential (-40 mV) for L-type Ca^{2+} channels whereas membrane potential is hyperpolarized (-60 to -75 mV) in non-pressurized isolated resistance vessels, including rat afferent arterioles.[25] Higher concentrations of agonists are therefore required to activate Ca^{2+} entry and vasoconstriction in isolated arterioles.

ET-1- and Ang II-induced LC_{20} phosphorylation

To gain insight into the molecular basis of the different vasoconstrictor and vasodilator responses to ET-1 and Ang II, LC_{20} phosphorylation was measured in isolated afferent arterioles in response to various concentrations of agonist. Most interestingly, ET-1 induced LC_{20} diphosphorylation in addition to monophosphorylation in a concentration-dependent manner (Figure 4A, B). The level of LC_{20} monophosphorylation reached a plateau of 41.1 ± 3.0% (n = 7) at 10 nmol/L ET-1, but diphosphorylation increased the total phosphorylation level to 59.8 ± 3.1% (n = 7) at 10 nmol/L ET-1 and 69.7 ± 4.0% (n = 5) at 100 nmol/L ET-1. The time-courses of LC_{20} mono- and diphosphorylation

in the afferent arteriole in response to ET-1 treatment (10 nmol/L) are shown in Figure 4C and D. LC_{20} monophosphorylation increased rapidly following the application of ET-1, reaching a steady-state level of 46.2 ± 2.7% (n = 4) within 60 s. LC_{20} diphosphorylation increased more slowly, reaching a maximum level of 15.7 ± 2.2% (n = 8) within 5 min. On the other hand, Ang II induced exclusively LC_{20} monophosphorylation in a concentration- and time-dependent manner (Figure 5), reaching a plateau level of phosphorylation of 38.9 ± 3.0% (n = 17) at 10 nmol/L, consistent with our earlier studies of Ang II-induced LC_{20} phosphorylation.[21] Comparison of the effects of ET-1 and Ang II suggested a unique LC_{20} phosphorylation response to ET-1, i.e. phosphorylation occurs at two sites in LC_{20} in response to ET-1. Since diphosphorylation is associated with slower rates of dephosphorylation and relaxation,[18] this difference could contribute to the difference in vasodilation observed in response to the two agonists (Figure 2).

Identification of the LC_{20} diphosphorylation sites

The sites of phosphorylation in LC_{20} in response to ET-1 treatment were identified by Phos-tag SDS-PAGE followed by western blotting with a diphosphospecific antibody that recognizes LC_{20} only when phosphorylated at both Thr18 and Ser19 (Figure 6). Triton-skinned, microcystin-treated rat caudal arterial smooth muscle was used as a positive control for LC_{20} diphosphorylation.[18,21,26,27]

Western blotting with an antibody to LC_{20} that recognizes all forms of the protein (phosphorylated and unphosphorylated) revealed three separated bands in ET-1-treated afferent arterioles, which co-migrated with the three bands in microcystin-treated rat caudal arterial smooth muscle strips (Figure 6, left panel). The diphosphospecific antibody recognized only the slowest migrating band in the afferent arteriole treated with ET-1, and rat caudal artery treated with microcystin (Figure 6, right panel). Under basal (unstimulated) conditions, only unphosphorylated LC_{20} was detected in the afferent arteriole (Figure 6). We conclude that ET-1 induces phosphorylation of LC_{20} at both Thr18 and Ser19 in the afferent arteriole.

ET-1-induced LC_{20} diphosphorylation at these specific sites was confirmed using the proximity ligation assay.[28] We chose this assay rather than regular immunostaining with antibody specific for diphosphorylated LC_{20} due to its sensitivity, specificity and high signal-to-noise ratio. Afferent arterioles under basal conditions or following treatment with ET-1 or Ang II were fixed, permeabilized and incubated with two primary antibodies: mouse monoclonal anti-LC_{20} and rabbit polyclonal anti-pT18,pS19-LC_{20}. Subsequent addition of secondary antibodies to mouse and rabbit IgGs conjugated to paired oligonucleotides, followed by rolling circle DNA amplification enabled the detection of LC_{20} diphosphorylation *in situ* using fluorescently-labeled complementary oligonucleotides. Little fluorescence staining was observed in control, untreated afferent arterioles or

in arterioles treated with Ang II (Figure 7). On the other hand, strong fluorescent signals were observed in the smooth muscle cells following ET-1 treatment (Figure 7). This confirmed that diphosphorylation of LC_{20} at Thr18 and Ser19 occurs in afferent arterioles in response to ET-1, but not Ang II treatment.

Effects of kinase inhibitors on ET-1-induced LC_{20} phosphorylation

Selective inhibitors of ROCK (H1152) and MLCK (ML7) were used to assess the involvement of these kinases in LC_{20} mono- and diphosphorylation induced by ET-1. Inhibition of ROCK by H1152 (1 μmol/L) significantly reduced ET-1-induced LC_{20} monophosphorylation from 42.3 ± 1.1% (*n* = 23) to 32.3 ± 9.3% (*n* = 3) and diphosphorylation from 14.9 ± 1.2% (*n* = 23) to 3.4 ± 2.4% (*n* = 3) (Figure 8A). Similarly, inhibition of MLCK by ML7 (10 μmol/L) significantly reduced ET-1-induced LC_{20} monophosphorylation from 42.3 ± 1.1% (*n* = 23) to 23.6 ± 3.5% (*n* = 7) and diphosphorylation from 14.9 ± 1.2% (*n* = 23) to 2.6 ± 0.8% (*n* = 7) (Figure 8A). These results implicate both MLCK and ROCK in ET-1-induced afferent arteriolar vasoconstriction.

Effects of ET_B receptor agonist and antagonist and ET_A receptor antagonist on ET-1-induced LC_{20} phosphorylation

Two ET-1 receptors have been identified: ET_A and ET_B.[9] We used a receptor-specific agonist and

antagonists to investigate which receptor mediates ET-1-induced LC_{20} diphosphorylation (Figure 8B). ET-1-induced LC_{20} diphosphorylation was abolished by pre-treatment with the ET_B receptor-specific antagonist BQ788 (1 μmol/L), with a significant reduction in the LC_{20} monophosphorylation level. The ET_B receptor-specific agonist sarafotoxin 6c (100 nmol/L) induced both LC_{20} mono- and diphosphorylation (Figure 8B) to levels approaching those observed with ET-1 itself (Figures 4, 8A and 8B), suggesting that activation of the ET_B receptor by ET-1 is coupled to LC_{20} diphosphorylation. Vasodilation following washout of sarafotoxin 6c was slow, and comparable to that following washout of ET-1 (Figure S1), consistent with delayed vasorelaxation due to LC_{20} diphosphorylation. Furthermore, the ET_A receptor antagonist BQ123 (1 μmol/L) had no effect on ET-1-induced LC_{20} diphosphorylation (Figure 8B). We also investigated the effect of BQ788 on the time course of vasodilation following removal of ET-1, and found that blockade of the ET_B receptor resulted in a significantly reduced rate of vasorelaxation following washout of ET-1 (Figure S2). Since ET_B receptors in vascular smooth muscle cells and endothelial cells have opposing vasoconstrictor and vasodilator effects, respectively, the slower rate of vasodilation following treatment with BQ788 could be due to inhibition of endothelial NO production. This conclusion was supported by the observation that inhibition of eNOS prolonged the vasodilatory response upon removal of ET-1 (Figure S3) but

had no effect on the BQ788-induced prolongation of vasodilation (Figure S4). In contrast, L-NAME prolonged the vasodilator response of arterioles pre-treated with BQ123 and constricted with ET-1 (Fig. S5), consistent with the fact that ET_A receptors are not coupled to NO production.

DISCUSSION

Ang II is a renal-selective vasoconstrictor that contributes to renal vascular resistance under normal physiological conditions and thereby plays an important role in modulating renal hemodynamics.[29] On the other hand, ET-1 is a renal vasoconstrictor that does not contribute to renal vascular resistance under normal physiological conditions, but is implicated in abnormal renal vasoconstriction in pathological states such as acute renal insufficiency and chronic kidney disease.[30] The vasoconstrictor responses to these two agonists and the vasodilation following their washout differ significantly

(Figures 1 and 2). This correlates with their distinct effects on renal perfusate flow: bolus administration of Ang II causes a transient decrease, whereas ET-1 induces a sustained decrease in renal perfusate flow.[4] We considered the possibility that these differences may reflect differences in LC_{20} phosphorylation, the fundamental mechanism for activation of smooth muscle contraction.[16] Ang II induced LC_{20} phosphorylation exclusively at Ser19, the MLCK site (Figure 5), which can be explained by a combination of activation of MLCK by increased $[Ca^{2+}]_i$, due primarily to Ca^{2+} entry via voltage-gated Ca^{2+} channels[25,31], and Ca^{2+} sensitization via activation of the ROCK pathway leading to MLCP inhibition (Supplemental Figure S6 and [32]). The slower rate of vasoconstriction in response to ET-1 compared to Ang II (Figure 1) could be explained by a smaller increase in $[Ca^{2+}]_i$ and/or a slower rate of increase in $[Ca^{2+}]_i$.

Most interestingly, we found that ET-1, unlike Ang II, induced phosphorylation of LC_{20} at both Ser19 and Thr18 (Figures 4, 6 and 7). ET-1 elicited an increase in $[Ca^{2+}]_i$ (Figure 3C and D), again primarily due to Ca^{2+} entry via voltage-gated Ca^{2+} channels,[4] suggesting that, like Ang II, ET-1 leads to activation of MLCK and inhibition of MLCP, resulting in phosphorylation of LC_{20} at Ser19 by MLCK. These effects are likely mediated by the ET_A receptor.[9] It is important to note however that, although Ca^{2+} channel blockade diminished the ET-1-mediated increase in $[Ca^{2+}]_i$, the vasoconstrictor response of the afferent arteriole to ET-1 is relatively refractory to Ca^{2+} channel blockade (Figure 3A and B and

[33]), a finding consistent with the involvement of a second, Ca^{2+}-independent pathway. In support of this conclusion, pre-treatment with staurosporine was shown to enhance the sensitivity of ET-1-induced afferent arteriolar vasoconstriction to the dihydropyridine isradipine, which led the authors to conclude that ET-1-induced vasoconstriction requires activation of a staurosporine-sensitive kinase in addition to activation of voltage-gated Ca^{2+} channels.[33] At that time, staurosporine was thought to be a selective protein kinase C inhibitor, but is now known to be a non-selective kinase inhibitor.[34]

Since MLCP inhibition by microcystin causes LC_{20} diphosphorylation in vascular smooth muscles,[18,26,27] we had postulated that strong inhibition of MLCP by activation of the RhoA/ROCK pathway may be involved in the ET-1-induced LC_{20} diphosphorylation. However, inhibition of ROCK by H1152 did not abolish the ET-1-induced diphosphorylation, although it did significantly reduce both mono- and diphosphorylation levels (Figure 8A). Inhibition of MLCK by ML7 also failed to abolish LC_{20} mono- and diphosphorylation (Figure 8A). These results suggest that a signaling pathway other than MLCK activation or MLCP inhibition by ROCK must be involved in the ET-1-induced LC_{20} phosphorylation response in the afferent arteriole, consistent with the inability of MLCK to phosphorylate LC_{20} at Thr18 under physiological conditions.[18] The time-course of ET-1-induced LC_{20} phosphorylation displayed a rapid increase in monophosphorylation (within 30 - 60 s) and a slower

increase in diphosphorylation (5 min) (Figure 4C, D). Since ILK and ZIPK phosphorylate both sites,[19,35] we conclude that at least two distinct kinase pathways are involved in ET-1-induced LC_{20} diphosphorylation: activation of Ca^{2+}-dependent MLCK and concomitant inhibition of MLCP, leading to monophosphorylation at Ser19, and activation of Ca^{2+}-independent ILK and/or ZIPK, leading to phosphorylation at Thr18 and further phosphorylation at Ser19 (Figure 9A). The Ca^{2+}-independent pathway may contribute to the observed dissociation between changes in $[Ca^{2+}]_i$ and tone in response to Ca^{2+} channel blockade (Figure 3).

Ang II, on the other hand, did not induce LC_{20} diphosphorylation in afferent arterioles (Figure 5). The contractile response to Ang II can, therefore, be explained by activation of AT_1 receptors[5] leading to an increase in $[Ca^{2+}]_i$, activation of MLCK and phosphorylation of LC_{20} at Ser19 (Figure 9B). This is consistent with the earlier demonstration that, in the afferent arteriole at an intraluminal pressure of 80 mm Hg, Ang II elicits membrane depolarization from -40 ± 2 mV (near the activation threshold for L-type Ca^{2+} channels) to -29 ± 2 mV and Ca^{2+} entry via voltage-gated Ca^{2+} channels, which are associated with a reduction in arteriolar diameter from 13 ± 1 μm to 8 ± 1 μm.[25,31] The inhibition of Ang II-induced LC_{20} phosphorylation by ROCK inhibition (Supplemental Figure S6) indicates that Ca^{2+} sensitization also plays a significant role in the contractile response to Ang II, i.e. AT_1 receptor activation is also coupled to activation of $G_{12/13}$, leading to RhoA and ROCK activation, inhibition of

MLCP and increased LC_{20} phosphorylation at Ser19 (Figure 9B).

Both ET_A and ET_B receptors are expressed in the smooth muscle of rat afferent arterioles[9] and contribute to the contractile response of this vessel.[13] Selective blockade of ET_B receptors with BQ788 abolished LC_{20} diphosphorylation (Figure 8B). Furthermore, selective activation of ET_B receptors with sarafotoxin 6c induced LC_{20} mono- and diphosphorylation (Figure 8B). In this case, the monophosphorylated LC_{20} is likely a mixture of LC_{20} monophosphorylated at Thr18 and LC_{20} monophosphorylated at Ser19. These results strongly suggest that activation of ET_B receptors leads to LC_{20} diphosphorylation, which most likely occurs via activation of ILK and/or ZIPK. ET-1 failed to induce LC_{20} diphosphorylation in rat caudal arterial smooth muscle strips (data not shown) in which ET_A is known to be the predominant contractile endothelin receptor,[36] supporting the conclusion that ET_B receptors are responsible for ET-1-induced LC_{20} diphosphorylation in the rat afferent arteriole. This conclusion is supported by our observation that the ET_A receptor antagonist BQ123 did not affect ET-1-induced LC_{20} diphosphorylation (Figure 8B).

A few examples of LC_{20} diphosphorylation have been reported in non-diseased smooth muscle tissues in response to neural or carbachol stimulation of bovine tracheal smooth muscle[37,38] and prostaglandin $F_{2\alpha}$ treatment of rabbit thoracic aorta.[39,40] LC_{20} diphosphorylation has, however, been observed more frequently in disease states associated with smooth muscle hypercontractility: intimal

hyperplasia,[41] coronary arterial vasospasm,[42,43] cerebral vasospasm[44,45] and hypertension.[46] We showed recently that the functional effect of LC_{20} diphosphorylation is to slow the rate of dephosphorylation and relaxation compared to the situation in which LC_{20} is phosphorylated exclusively at Ser19.[18] This could explain, at least in part, the differences in the time-courses of vasodilation following washout of Ang II and ET-1 (Figure 2), recognizing that the slow dissociation rate of ET-1 from its receptors is likely also to be a contributing factor.[47-49] Given that ET-1 increases in ischemic kidney,[50] ET-1-induced LC_{20} diphosphorylation and consequent prolonged contraction of the pre-glomerular vessels may contribute to ischemia/reperfusion-induced acute renal failure. Several studies have suggested that endothelial ET_B receptors are protective in a number of renal disorders, including renal failure.[51,52] Thus, while endothelial ET_B receptors may offer renal protection via the stimulation of NOS,[51] the activation of ET_B receptors on the afferent arteriolar myocytes might contribute to the abnormal vasoconstriction or vasospasm associated with recovery.

METHODS

Available in the Supplementary Material online.

DISCLOSURE

All the authors declared no competing interests.

SUPPLEMENTARY MATERIAL

Methods.

Table S1. Afferent arteriolar diameters prior to and following vasoconstriction, and following vasodilation after agonist washout in SD rats.

Figure S1. Kinetics of renal arteriolar vasodilation following washout of ET-1 or sarafotoxin 6c in SD rats.

Figure S2. Kinetics of renal arteriolar vasodilation following washout of ET-1 with or without BQ788 in SD rats.

Figure S3. Kinetics of renal arteriolar vasodilation following washout of ET-1 with or without L-NAME in SD rats.

Figure S4. Kinetics of renal arteriolar vasodilation following washout of BQ788 and ET-1 with or without L-NAME in SD rats.

Figure S5. Kinetics of renal arteriolar vasodilation following washout of BQ123 and ET-1 with or without L-NAME in SD rats.

Figure S6. Effect of ROCK inhibition on Ang II-induced LC_{20} phosphorylation.

Supplementary information is available at *Kidney International*'s website.

REFERENCES

1. Gomez-Garre D, Largo R, Liu XH, *et al*. An orally active ET_A/ET_B receptor antagonist ameliorates proteinuria and glomerular lesions in rats with proliferative nephritis. *Kidney Int* 1996; **50**: 962-972.
2. Orth SR, Esslinger JP, Amann K, *et al*. Nephroprotection of an ET_A-receptor blocker (LU 135252) in salt-loaded uninephrectomized stroke-prone spontaneously hypertensive rats. *Hypertension.* 1998; **31**: 995-1001.
3. Wilhelm SM, Stowe NT, Robinson AV, *et al*. The use of the endothelin receptor antagonist, tezosentan, before and after renal ischemia protects renal function. *Transplantation.* 2001; **71**: 211-216.

4. Loutzenhiser R, Epstein M, Hayashi K, *et al*. Direct visualization of effects of endothelin on the renal microvasculature. *Am J Physiol Renal Physiol* 1990; **258**: F61-F68.

5. Edwards RM, Aiyar N. Angiotensin II receptor subtypes in the kidney. *J Am Soc Nephrol* 1993; **3**: 1643-1652.

6. Kon V, Yoshioka T, Fogo A, *et al*. Glomerular actions of endothelin *in vivo*. *J Clin Invest* 1989; **83**: 1762-1767.

7. Claria J, Jimenez W, La Villa G, *et al*. Effects of endothelin on renal haemodynamics and segmental sodium handling in conscious rats. *Acta Physiol Scand* 1991; **141**: 305-308.

8. Harris PJ, Zhuo J, Mendelsohn FA, *et al*. Haemodynamic and renal tubular effects of low doses of endothelin in anaesthetized rats. *J Physiol* 1991; **433**: 25-39.

9. Wendel M, Knels L, Kummer W, *et al*. Distribution of endothelin receptor subtypes ET_A and ET_B in the rat kidney. *J Histochem Cytochem* 2006; **54**: 1193-1203.

10. Lanese DM, Conger JD. Effects of endothelin receptor antagonists on cyclosporine-induced vasoconstriction in isolated rat renal arteries. *J Clin Invest* 1993; **91**: 2144-2149.

11. Wellings RP, Corder R, Warner TD, *et al*. Evidence from receptor antagonists of an important role for the ET_B receptor-mediated vasoconstrictor effects of endothelin-1 in the rat kidney. *Br J Pharmacol* 1994; **111**: 515-520.

12. Endlich K, Hoffend J, Steinhausen M. Localization of endothelin ET_A and ET_B receptor-mediated constriction in the renal microcirculation of rats. *J Physiol* 1996; **497**: 211-218.

13. Inscho EW, Imig JD, Cook AK, *et al*. ET_A and ET_B receptors differentially modulate afferent and efferent arteriolar responses to endothelin. *Br J Pharmacol* 2005; **146**: 1019-1026.

14. Ekelund U, Adner M, Edvinsson L, *et al*. Effects of selective ET_B-receptor stimulation on arterial, venous and capillary functions in cat skeletal muscle. *Br J Pharmacol* 1994; **112**: 887-894.

15. Yanagisawa M, Kurihara H, Kimura S, *et al*. A novel potent vasoconstrictor peptide produced by vascular endothelial cells. *Nature* 1988; **332**: 411-415.

16. Allen BG, Walsh MP. The biochemical basis of the regulation of smooth-muscle contraction. *Trends Biochem Sci* 1994; **19**: 362-368.

17. Somlyo AP, Somlyo AV. Ca^{2+} sensitivity of smooth muscle and non-muscle myosin II: modulated by G proteins, kinases and myosin phosphatase. *Physiol Rev* 2003; **83**: 1325-1358.

18. Sutherland C, Walsh MP. Myosin regulatory light chain diphosphorylation slows relaxation of arterial smooth muscle. *J Biol Chem* 2012; **287**: 24064-24076.

19. Deng JT, Van Lierop JE, Sutherland C, *et al*. Ca^{2+}-independent smooth muscle contraction. A novel function for integrin-linked kinase. *J Biol Chem* 2001; **276**: 16365-16373.

20. Moffat LD, Brown SBA, Grassie ME, *et al*. Chemical genetics of zipper-interacting protein kinase

reveal myosin light chain as a *bona fide* substrate in permeabilized arterial smooth muscle. *J Biol Chem* 2011; **286**: 36978-36991.

21. Takeya K, Loutzenhiser K, Shiraishi M, *et al*. A highly sensitive technique to measure myosin regulatory light chain phosphorylation: the first quantification in renal arterioles. *Am J Physiol Renal Physiol* 2008; **294**: F1487-F1492.
22. Shiraishi M, Wang X, Walsh MP, *et al*. Myosin heavy chain isoform expression in renal afferent and efferent arterioles: relationship to contractile kinetics and function. *FASEB J* 2003; **17**: 2284-2286.
23. Shiraishi M, Loutzenhiser RD, Walsh MP. A highly sensitive method for quantification of myosin light chain phosphorylation by capillary isoelectric focusing with laser-induced fluorescence detection. *Electrophoresis* 2005; **26**: 571-580.
24. Kinoshita E, Kinoshita-Kikuta E, Takiyama K, *et al*. Phosphate-binding tag, a new tool to visualize phosphorylated proteins. *Mol Cell Proteomics* 2006; **5**: 749-757.
25. Loutzenhiser R, Chilton L, Trottier G. Membrane potential measurements in renal afferent and efferent arterioles: actions of angiotensin II. *Am J Physiol Renal Physiol* 1997; **273**: F307-F314.
26. Weber LP, Van Lierop JE, Walsh MP. Ca^{2+}-independent phosphorylation of myosin in rat caudal artery and chicken gizzard myofilaments. *J Physiol* 1999; **516**: 805–824.
27. Wilson DP, Sutherland C, Borman MA, *et al*. Integrin-linked kinase is responsible for

Ca^{2+}-independent myosin diphosphorylation and contraction of vascular smooth muscle. *Biochem J* 2005; **392**: 641–648.

28. Söderberg O, Gullberg M, Jarvius M, *et al*. Direct observation of individual endogenous protein complexes in situ by proximity ligation. *Nat Methods* 2006; **3**: 995-1000.
29. Navar LG, Gilmore JP, Joyner WL, *et al*. Direct assessment of renal microcirculatory dynamics. *Fed Proc* 1986; **45**: 2851-2861.
30. Vachiéry J-L, Davenport A. The endothelin system in pulmonary and renal vasculopathy: les liaisons dangereuses. *Eur Respir Rev* 2009; **18**: 260-271.
31. Loutzenhiser K, Loutzenhiser R. Angiotensin II-induced Ca^{2+} influx in renal afferent and efferent arterioles: differing roles of voltage-gated and store-operated Ca^{2+} entry. *Circ Res* 2000; **87**: 551-557.
32. Nakamura A, Hayashi K, Ozawa Y, *et al*. Vessel- and vasoconstrictor-dependent role of Rho/Rho kinase in renal microvascular tone. *J Vasc Res* 2003; **40**: 244-251.
33. Takenaka T, Forster H, Epstein M. Protein kinase C and calcium channel activation as determinants of renal vasoconstriction by angiotensin II and endothelin. *Circ Res* 1993; **73**: 743-750.
34. Karaman MW, Herrgard S, Treiber DK, *et al*. A quantitative analysis of kinase inhibitor selectivity. *Nat Biotech* 2008; **26**: 127-132.
35. Niiro N, Ikebe M. Zipper-interacting protein kinase induces Ca^{2+}-free smooth muscle contraction via

myosin light chain phosphorylation. *J Biol Chem* 2001; **276**: 29567-29574.

36. Adner M, Uddman E, Cardell LO, *et al*. Regional variation in appearance of vascular contractile endothelin-B receptors following organ culture. *Cardiovasc Res* 1998; **37**: 254-262.
37. Miller-Hance WC, Miller JR, Wells JN, *et al*. Biochemical events associated with activation of smooth muscle contraction. *J Biol Chem* 1988; **263**: 13979-13982.
38. Colburn JC, Michnoff CH, Hsu LC, *et al*. Sites phosphorylated in myosin light chain in contracting smooth muscle. *J Biol Chem* 1988; **263**: 19166-19173.
39. Seto M, Sasaki Y, Sasaki Y. Stimulus-specific patterns of myosin light chain phosphorylation in smooth muscle of rabbit thoracic aorta. *Pflügers Arch* 1990; **415**: 484-489.
40. Seto M, Sasaki Y, Sasaki Y, *et al*. Effect of HA1077, protein kinase inhibitor, on myosin phosphorylation and tension in smooth muscle. *Eur J Pharmacol* 1991; **195**: 267-272.
41. Seto M, Yano K, Sasaki Y, *et al*. Intimal hyperplasia enhances myosin phosphorylation in rabbit carotid artery. *Exp Mol Pathol* 1993; **58**: 1-13.
42. Katsumata N, Shimokawa H, Seto M, *et al*. Enhanced myosin light chain phosphorylations as a central mechanism for coronary artery spasm in a swine model with interleukin-1β. *Circulation* 1997; **96**: 4357-4363.
43. Shimokawa H, Seto M, Katsumata N, *et al*. Rho-kinase-mediated pathway induces enhanced myosin

light chain phosphorylations in a swine model of coronary artery spasm. *Cardiovasc Res* 1999; **43**: 1029-1039.

44. Harada T, Seto M, Sasaki Y, *et al*. The time course of myosin light chain phosphorylation in blood-induced vasospasm. *Neurosurgery* 1995; **36**: 1178-1182.
45. Obara K, Nishizawa S, Koide M, *et al*. Interactive role of protein kinase C-δ with Rho-kinase in the development of cerebral vasospasm in a canine two-hemorrhage model. *J Vasc Res* 2005; **41**: 67-76.
46. Cho Y-E, Ahn D-S, Morgan KG, *et al*. Enhanced contractility and myosin phosphorylation induced by Ca^{2+}-independent MLCK activity in hypertensive rats. *Cardiovasc Res* 2011; **91**: 162-170.
47. Hemsén A, Franco-Cereceda A, Matran R, *et* al. Occurrence, specific binding sites and functional effects of endothelin in human cardiopulmonary tissue. *Eur J Pharmacol* 1990;**191**: 319-328.
48. Hemsén A, Larsson O, Lundberg JM. Characteristics of endothelin A and B binding sites and their vascular effects in pig peripheral tissue. *Eur J Pharmacol* 1991;**208**: 313-322.
49. Bolger GT, Liard F, Garneau M, *et al*. Characterization of intestinal smooth muscle responses and binding sites for endothelin. *Can J Physiol Pharmacol* 1991; **70**: 377-384,
50. Wilhelm SM, Simonson MS, Robinson AV, *et al*. Endothelin up-regulation and localization following renal ischemia and reperfusion. *Kidney Int* 1999; **55**: 1011-1018.
51. Nishida M, Ieshima M, Konishi F, *et al*. Role of endothelin B receptor in the pathogenesis of ischemic

acute renal failure. *J Cardiovasc Pharmacol* 2002; **40**: 586-593.

52. Ohkita M, Takaoka M, Matsumura Y. Drug discovery for overcoming chronic kidney disease (CKD): The endothelin ET_B receptor / nitric oxide system functions as a protective factor in CKD. *J Pharmacol Sci* 2009; **109**: 7-13.

TITLES AND LEGENDS

Figure 1. Kinetics of renal arteriolar vasoconstriction in response to Ang II and ET-1 in SD rats. (**A**) The time-courses of 0.1 nmol/L Ang II- and ET-1-induced vasoconstriction are shown as mean values ± S.E.M. (n = 5 for Ang II and n = 8 for ET-1), the thin lines depicting the S.E.M.. The ET-1-evoked maximal vasoconstriction was stable for at least 5 min. (**B**) Values of $t_{1/2}$ (time to half-maximal vasoconstriction) following application of 0.1 nmol/L Ang II (n = 5) or ET-1 (n = 8).

Figure 2. Kinetics of renal arteriolar vasodilation following washout of Ang II and ET-1 in SD

rats. (**A**) and (**C**) The time-courses of vasodilation following washout of 0.1 nmol/L Ang II and ET-1 are shown on long and short time-scales, respectively, as mean values ± S.E.M. (*n* = 5 for Ang II and *n* = 8 for ET-1), the thin lines depicting the S.E.M.. (**B**) Values of $t_{1/10}$ (time to 10% maximal dilation), $t_{1/2}$ (time to half-maximal vasodilation) and $t_{9/10}$ (time to 90% maximal dilation) following washout of Ang II (*n* = 5) or ET-1 (*n* = 8).

Figure 3. ET-1-induced afferent arteriolar vasoconstriction and increased $[Ca^{2+}]_i$, and the effect of voltage-gated Ca^{2+} channel blockade. (**A**) Representative trace showing the vasoconstrictor effect of ET-1 (0.1 nmol/L) on the renal afferent arteriole of SD rats *in situ* and the effect of subsequent application of diltiazem (1 and 10 μmol/L) in the continued presence of ET-1. Cumulative data are shown in (**B**) (*n* = 5). (**C**) Isolated Wistar rat afferent arterioles loaded with fura 2-AM were treated with ET-1 (10 nmol/L) and subsequently with diltiazem (1 and 10 μmol/L) in the continued presence of ET-1. Changes in $[Ca^{2+}]_i$ were followed by measuring $F_{340/380}$ ratio. Cumulative data are shown in (**D**) (*n* = 7). (**E**) Quantitative comparison of the effects of diltiazem on the ET-1-induced vasoconstriction (○) and $[Ca^{2+}]_i$ (●) (*n* = 5 for constriction and *n* = 7 for $[Ca^{2+}]_i$).

Figure 4. ET-1-induced LC_{20} phosphorylation in renal afferent arterioles of Wistar rats. (**A**) and

(**B**) Isolated afferent arterioles were treated with the indicated concentrations of ET-1 for 5 min. Phosphorylated and unphosphorylated forms of LC_{20} were separated by Phos-tag SDS-PAGE and detected by a 3-step western blotting procedure with anti-LC_{20}. A representative western blot is shown in (**A**) with cumulative quantitative data in (**B**). Data indicate the mean ± S.E.M. (*n* = 5 except for 10 nmol/L ET-1 where *n* = 7). (**C**) and (**D**) Time-courses of LC_{20} mono- and diphosphorylation in response to ET-1 (10 nmol/L). A representative western blot is shown in (**C**) with cumulative quantitative data in (**D**). Data indicate the mean ± S.E.M. (*n* = 4 except for 15 s, 45 s and 5 min where *n* = 3, 2 and 8, respectively). Percent phosphorylation was calculated from the following equations: % 1P-LC_{20} = [1P/(0P + 1P + 2P)] X 100%; % 2P-LC_{20} = [2P/(0P + 1P + 2P)] X 100%; % total P-LC_{20} = [(1P + 2P)/(0P + 1P + 2P)] X 100%.

Figure 5. Ang II-induced LC_{20} phosphorylation in renal afferent arterioles of Wistar rats. (**A**) and (**B**) Isolated afferent arterioles were treated with the indicated concentrations of Ang II for 5 min. Phosphorylated and unphosphorylated forms of LC_{20} were separated by Phos-tag SDS-PAGE and detected by a 3-step western blotting procedure with anti-LC_{20}. A representative western blot is shown in **A** with cumulative quantitative data in **B**. Data indicate the mean ± S.E.M. (*n* = 4 except for 0 and 10 nmol/L Ang II where *n* = 19 and 17, respectively). (**C**) Time-course of LC_{20} monophosphorylation

in response to Ang II (10 nmol/L). Data indicate the mean ± S.E.M. (*n* = 13 for time zero, *n* = 6 for 0.5, 1 and 2 min, and *n* = 5 for 5 and 10 min). Percent phosphorylation was calculated from the following equation: % 1P-LC_{20} = [1P/(0P + 1P)] X 100%. LC_{20} diphosphorylation was never observed in the afferent arteriole treated with Ang II.

Figure 6. Identification of the sites of phosphorylation in LC_{20} in response to ET-1. LC_{20} phosphorylation was analysed in untreated (lanes 2 and 5) and ET-1-treated (10 nmol/L for 5 min; lanes 3 and 6) Wistar rat afferent arterioles (AA) by Phos-tag SDS-PAGE and western blotting. Left panel: blot incubated with pan-LC_{20} antibody; right panel: identical blot incubated with anti-pT18,pS19-LC_{20}. Triton-skinned, microcystin (MC)-treated rat caudal artery (RCA) was included as a positive control since the three LC_{20} bands have been previously identified as labeled.[18]

Figure 7. Proximity ligation assay for LC_{20} diphosphorylation. Untreated Wistar rat afferent arterioles (control) and afferent arterioles treated with ET-1 or Ang II (10 nmol/L for 5 min) were fixed, permeabilized and incubated with pan-LC_{20} antibody and anti-pT18,pS19-LC_{20}. Bound antibodies in close proximity were detected by Cy3 staining. Panels show, from left to right, phase contrast images of the isolated arterioles, nuclear staining with DAPI, Cy3 fluorescence to illustrate LC_{20}

diphosphorylation, and merged images. Results are representative of 18 (control), 4 (ET-1) and 4 (Ang II) independent experiments.

Figure 8. Effects of ROCK and MLCK inhibition and ET_B receptor agonist and ET_A and ET_B receptor antagonist treatment on ET-1-induced LC_{20} mono- and diphosphorylation. (**A**) Isolated Wistar rat afferent arterioles were pre-treated with H1152 (1 μmol/L), ML7 (10 μmol/L) or vehicle for 5 min prior to stimulation with ET-1 (10 nmol/L). After 5 min of stimulation, tissues were harvested for analysis of LC_{20} phosphorylation by Phos-tag SDS-PAGE and western blotting with anti-LC_{20}. (**B**) Isolated afferent arterioles were untreated, treated with ET-1 (10 nmol/L) with or without pre-incubation for 5 min with BQ788 (1 μmol/L) or BQ123 (1 μmol/L), or treated with sarafotoxin 6c (100 nmol/L). After 5 min of stimulation, tissues were harvested for analysis of LC_{20} phosphorylation by Phos-tag SDS-PAGE and western blotting with anti-LC_{20}. Data indicate the mean ± S.E.M. (*n* values are indicated). Black bars represent LC_{20} monophosphorylation levels, white bars indicate diphosphorylation. Values were compared to those in the presence of ET-1 alone and statistically significant differences were identified by unpaired Student's t-test (*$p < 0.01$; **$p < 0.05$).

Figure 9. Proposed signaling pathways leading to ET-1-induced sustained vasoconstriction and

Ang II-induced transient vasoconstriction of the renal afferent arteriole. (**A**) ET-1, acting via ET_A receptors, triggers an increase in cytosolic free Ca^{2+} concentration ($[Ca^{2+}]_i$), largely through Ca^{2+} entry via voltage-gated Ca^{2+} channels (Ca_v), leading to binding of Ca^{2+} to calmodulin (CaM), activation of myosin light chain kinase (MLCK), phosphorylation of LC_{20} at Ser19 and cross-bridge cycling. Activation of ET_A receptors also induces inhibition of myosin light chain phosphatase (MLCP) via activation of the Rho-associated kinase (ROCK) pathway, leading to increased LC_{20} phosphorylation at Ser19 due to the increase in MLCK : MLCP activity ratio. MLCP inhibition unmasks basal activity of integrin-linked kinase (ILK) and/or zipper-interacting protein kinase (ZIPK) that phosphorylate LC_{20} at both Thr18 and Ser19. Activation of ET_B receptors in the vascular smooth muscle cells leads to activation of ILK and/or ZIPK (or possibly other kinase(s) capable of phosphorylating LC_{20} at Thr18 and Ser19). The rapid increase in Ser19 phosphorylation accounts for the initial phase of the contractile response to ET-1, while the slower diphosphorylation at Thr18 and Ser19, associated with reduced rates of LC_{20} dephosphorylation and relaxation,[18] can account for the sustained contractile response to ET-1 and prolonged contraction that occurs following removal of the stimulus. (**B**) Ang II, acting via AT_1 receptors, triggers an increase in $[Ca^{2+}]_i$, leading to activation of MLCK, phosphorylation of LC_{20} at Ser19 and cross-bridge cycling. AT_1 receptors are also coupled to the activation of ROCK, leading to inhibition of MLCP and enhanced LC_{20} phosphorylation. Removal of

the Ang II stimulus results in rapid vasodilation due to faster dephosphorylation of monophosphorylated LC_{20}.

Supplementary information

Endothelin-1, but not angiotensin II, induces afferent arteriolar myosin diphosphorylation

Kosuke Takeya, Xuemei Wang, Iris Kathol, Kathy Loutzenhiser, Rodger Loutzenhiser and Michael P. Walsh

METHODS

Measurement of afferent arteriolar diameter in the hydronephrotic kidney

All animal procedures were approved by the Animal Care and Use Committee of the Faculty of Medicine, University of Calgary and conformed to the standards of the Canadian Council on Animal Care. The isolated perfused hydronephrotic kidney is an established model that allows microscopic visualization of the renal microcirculation in a controlled *in vitro* setting.[1] The hydronephrotic kidney preparation (from 7- to 8-week old Sprague-Dawley (SD) rats; 200 - 250 g) and the perfusion apparatus used in this study have been described previously.[2-6] Vasoconstrictors were administered following pretreatment with ibuprofen (10 μmol/L) to eliminate effects of prostaglandins.[7] Afferent arteriolar diameters were measured by image processing as previously described.[4]

Isolation and stimulation of afferent arterioles

Renal afferent arterioles were isolated from 7- to 8-week old Wistar rats (200 - 250 g) as previously

described.[8,9] Since Cl^- current plays an important role in renal vascular contractions,[10] isethionate was included as a counterion to Na^+ to maintain the Cl^- concentration within the physiological range. Individual afferent arterioles, containing agarose to maintain physiological tension, were isolated using a dual pipette system with a Nikon TMS microscope and collected in ATM MEM in a BSA-coated culture dish. Three or four vessels were then transferred to tubes containing modified MEM (200 μL) containing (in mmol/L): 1.5 $CaCl_2$, 102.7 NaCl, 5.4 KCl, 1.7 NaH_2PO_4, 0.8 $MgSO_4$, 5 HEPES, 5.6 glucose, 1.0 sodium pyruvate, 26.2 $NaHCO_3$, 8 sodium isethionic acid, 1 x MEM vitamin solution, 1 x MEM non-essential amino acid solution and 1 x MEM amino acid solution. Ibuprofen (10 μmol/L) was added to eliminate the potential effect of prostaglandin E_2 on LC_{20} phosphorylation.[7] After 10 min in modified MEM at 37 ºC while gassing with 5% CO_2, 95% air, vessels were stimulated by adding 2 μL of 100-fold concentrated agonists and incubated at 37 ºC while gassing with 5% CO_2, 95% air. After incubation for 5 min, reactions were stopped by adding 1 mL of ice-cold 10% trichloroacetic acid (TCA), 10 mmol/L dithiothreitol (DTT) in acetone and samples processed for western blotting as previously described.[8] In some cases, vessels were treated with inhibitors for ≥ 10 min prior to stimulation.

It was necessary to use two different renal afferent arteriolar preparations in this study. The *in vitro* perfused hydronephrotic kidney preparation is suitable for measurement of vasoconstriction,

but it is unsuitable for LC_{20} phosphorylation measurements since it is not possible to quick-freeze the tissue and isolate the arteriole. On the other hand, isolated afferent arterioles are suitable for LC_{20} phosphorylation measurements, but do not permit measurements of vasoconstriction since the tiny vessels are floating in bathing solution in a test tube. The time-course of changes in LC_{20} phosphorylation after termination of stimulation unfortunately cannot be measured since the agonist cannot be washed out without losing the tiny vessels.

Measurement of $[Ca^{2+}]_i$

$[Ca^{2+}]_i$ was measured in isolated afferent arterioles loaded with fura 2-AM (5 μmol/L) as previously described.[9] Vessels were pretreated with ibuprofen (10 μmol/L) before the application of agonists to avoid the effects of prostaglandins.[7]

Quantification of LC_{20} phosphorylation

LC_{20} phosphorylation was measured by Phos-tag SDS-PAGE and a 3-step western blotting procedure as previously described.[8] The sensitivity of detection of the 3-step western blotting procedure[8] was enhanced by introducing Can Get Signal Immunoreaction Enhancer Solution (Toyobo Life Science, Japan). All forms of LC_{20} were detected using polyclonal rabbit anti-LC_{20} (Santa Cruz) and diphosphorylated forms of LC_{20} using polyclonal rabbit diphosphospecific anti-LC_{20} (Cell Signaling), which recognizes only LC_{20} that is phosphorylated at Thr18 and Ser19,[11] in

combination with chemiluminescence detection (LAS3000mini, Fujifilm) with the SuperSignal West Femto reagent (Pierce). Obtained images were analysed with Multi Gauge version 3.0 software (Fujifilm).

Proximity ligation assay

Diphosphorylated LC_{20} was detected in isolated vessels using the proximity ligation assay.[12] Isolated vessels in modified MEM containing $CaCl_2$ (1 mL) were placed on a round glass coverslip (18 mm) pretreated with Vectabond™ Reagent (Vector Laboratories) for maximal adhesion. After equilibration for 10 min at 37 ºC while gassing with 5% CO_2, 95% air, vessels were stimulated with ET-1 or Ang II (5 min) with or without pre-treatment with different blockers (5 min). Proteins were fixed in 1% formaldehyde for 10 min at room temperature. Agarose was removed with 60 μL agarase (2000 units/mL, Sigma from *Pseudomonas atlantica*) in 500 μL Hank's Balanced Salt Solution (HBSS) pH 6.0 (Gibco) warmed to 40 ºC for 10 min. Several rinses with HBSS were performed between each step. Vessels were skinned with 0.1% Triton X-100 in HBSS at room temperature. The PLA probe protocol with Duolink reagents (Olink Bioscience, Uppsala, Sweden) was followed: blocking, incubation with primary antibodies (mouse monoclonal anti-LC_{20} (Sigma) and rabbit polyclonal anti-pThr18,pSer19-LC_{20} (Cell Signaling)) at 1:200 overnight at 4 ºC, incubation with PLA Minus and Plus probes (secondary antibodies conjugated with

oligonucleotides), hybridization, ligation, amplification and detection. Imaging was performed with an Olympus Fluoview FV10i Confocal Microscope. This technique generates a fluorescent signal when pan-LC_{20} and diphosphospecific LC_{20} antibodies localize within ~ 40 nm of each other.[12]

Chemicals

ET-1, Ang II, ibuprofen and L-N^G-nitroarginine methyl ester (L-NAME) were purchased from Sigma. H1152, ML7, BQ788, BQ123 and sarafotoxin 6c were purchased from Calbiochem.

Data analysis

Values are presented as the mean ± S.E.M., with *n* indicating the number of animals and/or vessels used. Statistical analyses were performed with SigmaPlot and data were analysed by Student's *t* test, with $p < 0.05$ considered to indicate statistically significant differences.

REFERENCES

1. Loutzenhiser R, Hayashi K, Epstein M. Atrial natriuretic peptide reverses afferent arteriolar vasoconstriction and potentiates efferent arteriolar vasoconstriction in the isolated perfused rat kidney. *J Pharmacol Exp Ther* 1988; **246**: 522-528.

2. Loutzenhiser R, Chilton L, Trottier G. Membrane potential measurements in renal afferent and efferent arterioles: actions of angiotensin II. *Am J Physiol Renal Physiol* 1997; **273**: F307-F314.

3. Loutzenhiser R, Parker M. Hypoxia inhibits myogenic reactivity of renal afferent arterioles by activating ATP-sensitive potassium channels. *Circ Res* 1994; **74**: 861-869.

4. Loutzenhiser R. *In situ* studies of renal arteriolar function using the *in vitro* perfused hydronephrotic rat kidney, in *Symposium on Imaging*, eds. Sapin V, Weigmann T. Academic Press: San Diego, 1996, pp145-160.

5. Reslerova M, Loutzenhiser R. Divergent mechanisms of K_{ATP}-induced vasodilation in renal afferent and efferent arterioles: evidence for both L-type calcium channel-dependent and -independent actions of pinacidil. *Circ Res* 1995; **77**: 1114-1120.

6. Steinhausen M, Snoei H, Parekh N, *et al*. Hydronephrosis; a new method to visualize vas afferens, efferens and glomerular network. *Kidney Int* 1983; **23**: 794-806.

7. Tang L, Loutzenhiser K, Loutzenhiser R. Biphasic actions of prostaglandin E_2 on the renal afferent arteriole: role of EP_3 and EP_4 receptors. *Circ Res* 2000; **86**: 663-670.

8. Takeya K, Loutzenhiser K, Shiraishi M, *et al*. A highly sensitive technique to measure myosin regulatory light chain phosphorylation: the first quantification in renal arterioles. *Am J Physiol Renal Physiol* 2008; **294**: F1487-F1492.

9. Loutzenhiser K, Loutzenhiser R. Angiotensin II-induced Ca^{2+} influx in renal afferent and efferent arterioles: differing roles of voltage-gated and store-operated Ca^{2+} entry. *Circ Res* 2000; **87**: 551-

557.

10. Takenaka T, Kanno Y, Kitamura Y, *et al*. Role of chloride channels in afferent arteriolar constriction. *Kidney Int* 1996; **50**: 864-872.

11. Sutherland C, Walsh MP. Myosin regulatory light chain diphosphorylation slows relaxation of arterial smooth muscle. *J Biol Chem* 2012; **287**: 24064-24076.

12. Söderberg O, Gullberg M, Jarvius M, *et al*. Direct observation of individual endogenous protein complexes in situ by proximity ligation. *Nat Methods* 2006; **3**: 995-1000.

Supplemental Table 1 and Supplemental Figures S1 - S6

Table S1 | Afferent arteriolar diameters prior to and following vasoconstriction, and following vasodilation after agonist washout in SD rats

Treatment	Initial diameter (μm)	Following vasoconstriction (μm)	Following vasodilation (μm)	*n*
ET-1	19.0 ± 0.6	9.1 ± 0.5	18.3 ± 0.7	8
Ang II	17.7 ± 0.5	5.4 ± 0.6	17.6 ± 0.6	5
Sarafotoxin	20.4 ± 0.8	4.9 ± 1.2	19.0 ± 1.2	4
BQ788 + ET-1	18.3 ± 1.2	4.9 ± 0.3	18.8 ± 1.4	6
L-NAME + ET-1	17.8 ± 1.0	5.7 ± 0.3	18.1 ± 1.3	6
L-NAME + BQ788 + ET-1	20.3 ± 0.7	4.9 ± 0.6	19.9 ± 0.8	5
BQ123 + ET-1	19.0 ± 0.8	6.9 ± 0.3	18.5 ± 0.7	5
L-NAME + BQ123 + ET-1	18.9 ± 2.4	4.9 ± 0.4	18.7 ± 2.3	6

Renal arterial vasoconstriction was induced by ET-1 (0.1 nmol/L), Ang II (0.1 nmol/L) or sarafotoxin (100 nmol/L) in SD rats. In some cases vessels were pre-treated for ≥ 10 min with L-NAME (100 μmol/L) with or without BQ123 (1 μmol/L) or BQ788 (1 μmol/L). Afferent arteriolar diameter was measured *in situ* in the hydronephrotic kidney prior to addition of the contractile stimulus (initial diameter), following maximal constriction and again following vasodilation upon washout of agonist. Values indicate the mean diameter (μm) ± S.E.M. (*n* values indicated).

Supplemental Figure Legends

Figure S1. Kinetics of renal arteriolar vasodilation following washout of ET-1 or sarafotoxin 6c in SD rats. (**A**) Vasoconstriction was elicited by ET-1 (0.1 nmol/L) or sarafotoxin 6c (100 nmol/L). At time 0, agonists were washed out and afferent arteriolar diameter measured (shown as mean values ± S.E.M. (n = 8 for ET-1 and n = 4 for sarafotoxin 6c), the thin lines depicting the S.E.M.). (**B**) Values of $t_{1/10}$ (time to 10% maximal dilation), $t_{1/2}$ (time to half-maximal vasodilation) and $t_{9/10}$ (time to 90% maximal dilation) following washout of ET-1 (n = 8) or sarafotoxin 6c (n = 4). * indicates a statistically significant difference ($p < 0.04$). Diameters before addition of the stimulus, at maximal vasoconstriction and following vasodilation upon removal of the stimulus are provided in Table S1.

Figure S2. Kinetics of renal arteriolar vasodilation following washout of ET-1 with or without BQ788 in SD rats. (**A**) Vasoconstriction was elicited by ET-1 (0.1 nmol/L) in the absence or presence of BQ788 (1 µmol/L). Washout was initiated at time 0, and afferent arteriolar diameter measured (shown as mean values ± S.E.M. (n = 5), the thin lines depicting the S.E.M.). (**B**) Values of $t_{1/10}$, $t_{1/2}$ and $t_{9/10}$ following washout of ET-1 or BQ788 (n = 5). Error bars indicate S.E.M. and *$p < 0.001$. Diameters before addition of ET-1, at maximal vasoconstriction and following vasodilation upon washout of ET-1 are provided in Table S1.

Figure S3. Kinetics of renal arteriolar vasodilation following washout of ET-1 with or without L-NAME in SD rats. (**A**) The time-courses of vasodilation following washout of 0.1 nmol/L ET-1 with or without L-NAME (100 µmol/L) are shown as mean values ± S.E.M. (n = 6), the thin lines depicting the S.E.M.. (**B**) Values of $t_{1/10}$, $t_{1/2}$ and $t_{9/10}$ following washout of ET-1 or L-NAME + ET-1 (n = 6). Error bars indicate S.E.M. and *$p < 0.001$. Diameters before addition of ET-1, at maximal vasoconstriction and following vasodilation upon washout of ET-1 are provided in Table S1.

Figure S4. Kinetics of renal arteriolar vasodilation following washout of BQ788 and ET-1 with or without L-NAME in SD rats. (**A**) The time-courses of vasodilation following washout of 0.1 nmol/L ET-1 and 1 µmol/L BQ788 with or without L-NAME (100 µmol/L)

are shown as mean values ± S.E.M. (n = 6 for BQ788 + ET-1 and n = 5 for BQ788 + ET-1 + L-NAME), the thin lines depicting the S.E.M.. (**B**) Values of $t_{1/10}$, $t_{1/2}$ and $t_{9/10}$ following washout of BQ788 + ET-1 (n = 6) or BQ788 + ET-1 + L-NAME (n = 5). No significant differences ± L-NAME were observed ($p > 0.4$). Diameters before addition of ET-1, at maximal vasoconstriction and following vasodilation upon washout of ET-1 are provided in Table S1.

Figure S5. Kinetics of renal arteriolar vasodilation following washout of BQ123 and ET-1 with or without L-NAME in SD rats. (**A**) The time-courses of vasodilation following washout of 0.1 nmol/L ET-1 and 1 µmol/L BQ123 with or without L-NAME (100 µmol/L) are shown as mean values ± S.E.M. (n = 5 for BQ123 + ET-1 and n = 6 for BQ123 + ET-1 + L-NAME), the thin lines depicting the S.E.M.. (**B**) Values of $t_{1/10}$, $t_{1/2}$ and $t_{9/10}$ following washout of BQ123 + ET-1 (n = 5) or BQ123 + ET-1 + L-NAME (n = 6). Diameters before addition of ET-1, at maximal vasoconstriction and following vasodilation upon washout of ET-1 are provided in Table S1.

Figure S6. Effect of ROCK inhibition on Ang II-induced LC_{20} phosphorylation. Isolated Wistar rat afferent arterioles were pre-treated with Y27632 (3 µmol/L) or vehicle for 5 min prior to stimulation with Ang II (10 nmol/L). After 5 min of stimulation, tissues were harvested for analysis of LC_{20} phosphorylation by Phos-tag SDS-PAGE and western blotting with anti-LC_{20}. Data indicate the mean ± S.E.M. (n = 8). Values were compared to those in the presence of Ang II alone and statistically significant differences were identified by unpaired Student's t-test with $*p < 0.01$. In two additional experiments, H1152 (1 µmol/L) completely inhibited the Ang II-induced LC_{20} phosphorylation.

Figure S1

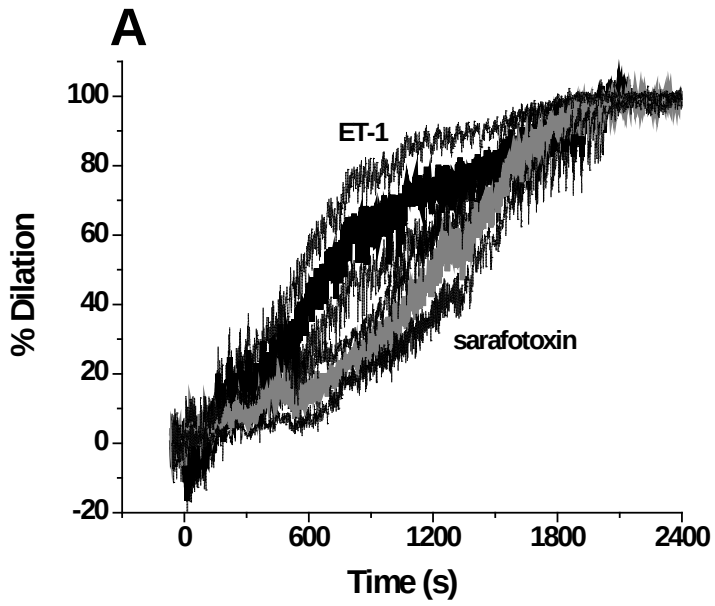
A
100
80
60
40
20
0
-20
% Dilation
ET-1
sarafotoxin
0
600
1200
1800
2400
Time (s)

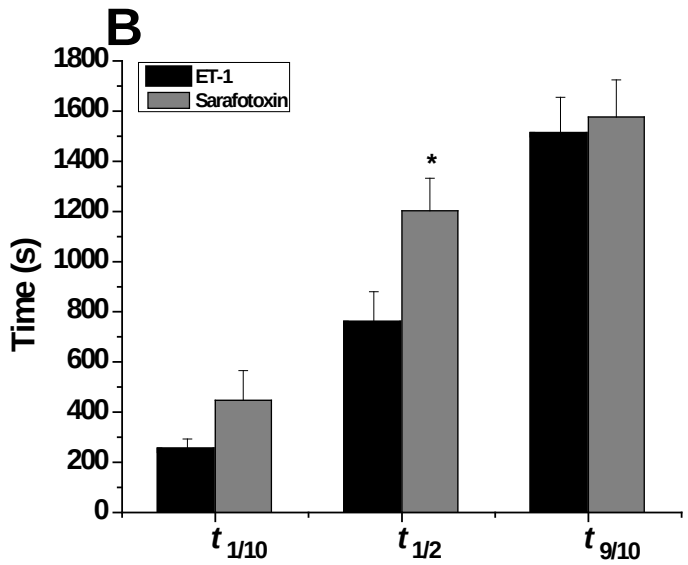
B
1800
1600
1400
1200
1000
800
600
400
200
0
Time (s)
ET-1
Sarafotoxin
*
t 1/10
t 1/2
t 9/10

Figure S2

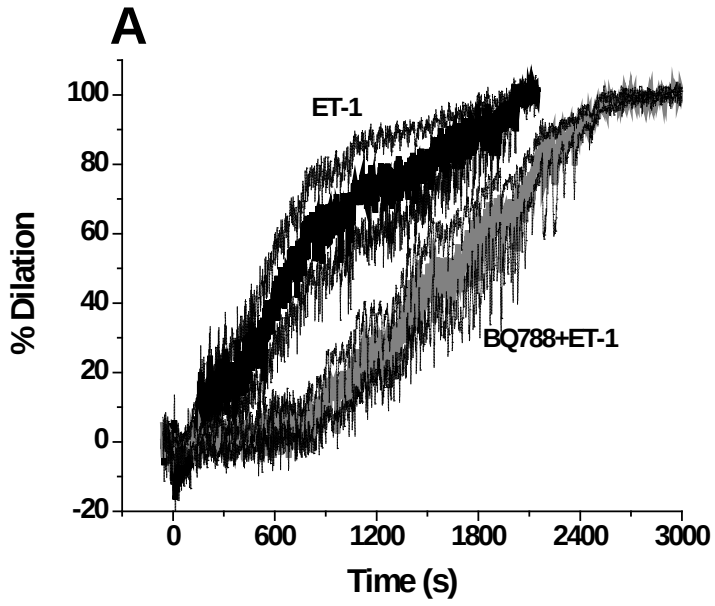
A
ET-1
BQ788+ET-1
% Dilation
Time (s)
100
80
60
40
20
0
-20
0
600
1200
1800
2400
3000

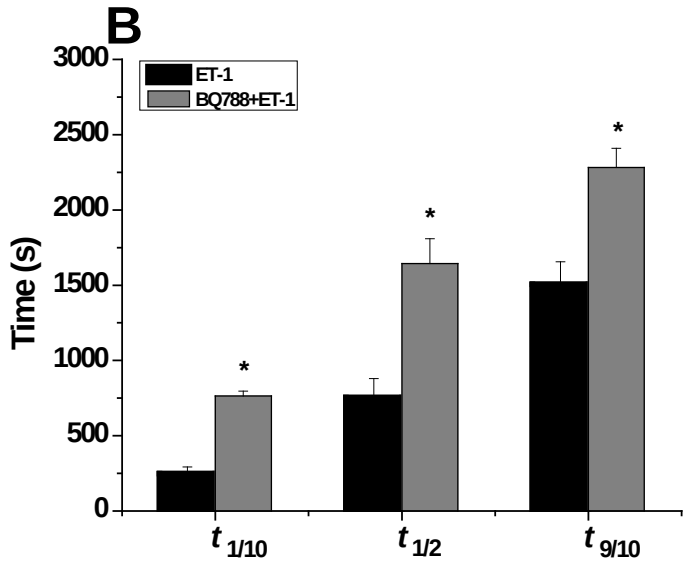
B
ET-1
BQ788+ET-1
Time (s)
3000
2500
2000
1500
1000
500
0
*
*
*
t 1/10
t 1/2
t 9/10

Figure S3

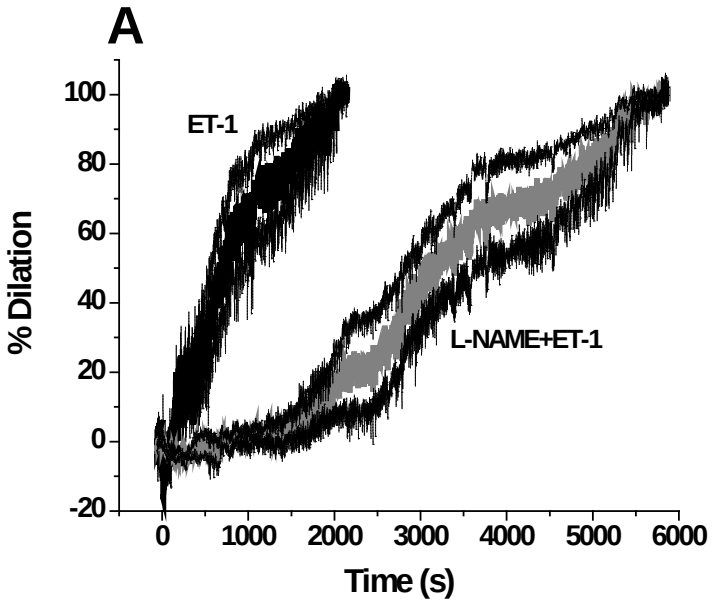
A
100
80
60
40
20
0
-20
% Dilation
ET-1
L-NAME+ET-1
0
1000
2000
3000
4000
5000
6000
Time (s)

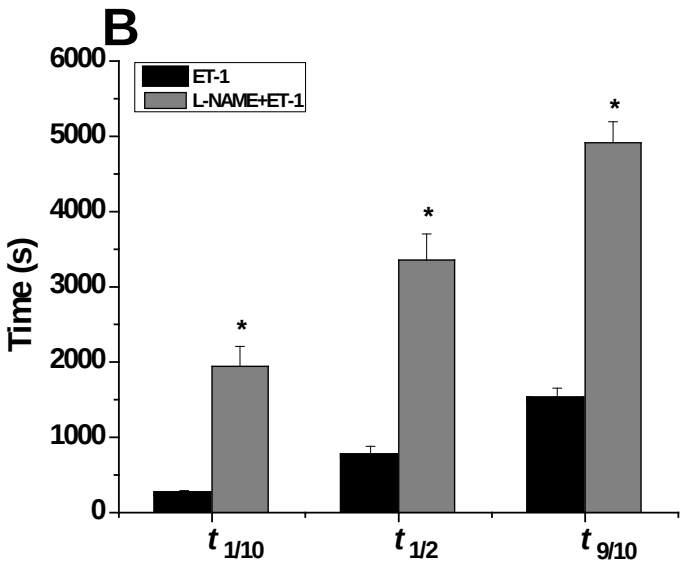
B
6000
5000
4000
3000
2000
1000
0
Time (s)
ET-1
L-NAME+ET-1
*
*
*
t 1/10
t 1/2
t 9/10

Figure S4

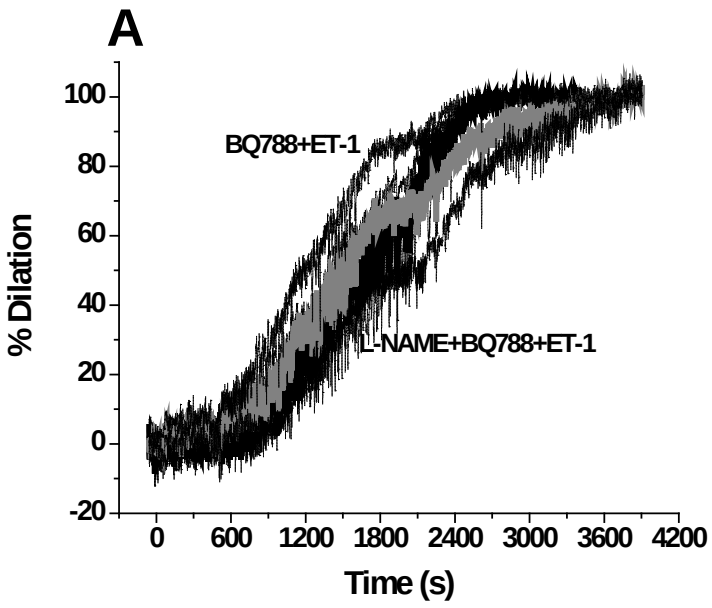
A
100
80
60
40
20
0
-20
% Dilation
BQ788+ET-1
L-NAME+BQ788+ET-1
0
600
1200
1800
2400
3000
3600
4200
Time (s)

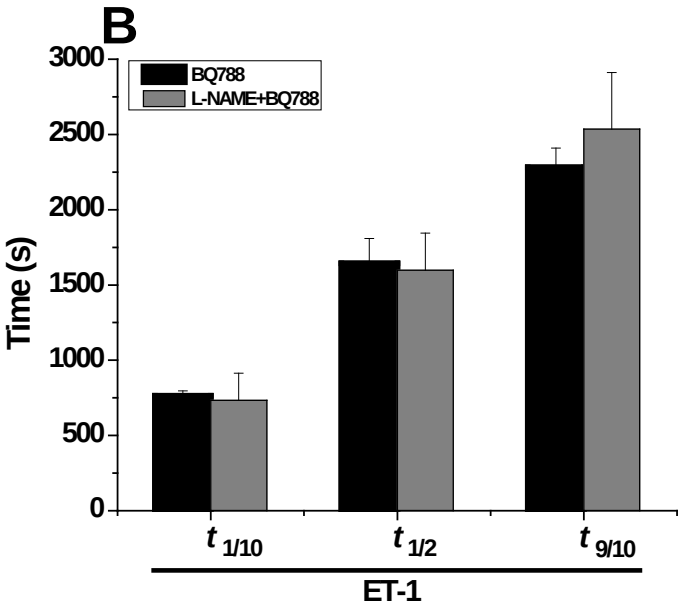
B
3000
2500
2000
1500
1000
500
0
Time (s)
BQ788
L-NAME+BQ788
t 1/10
t 1/2
t 9/10
ET-1

Figure S5

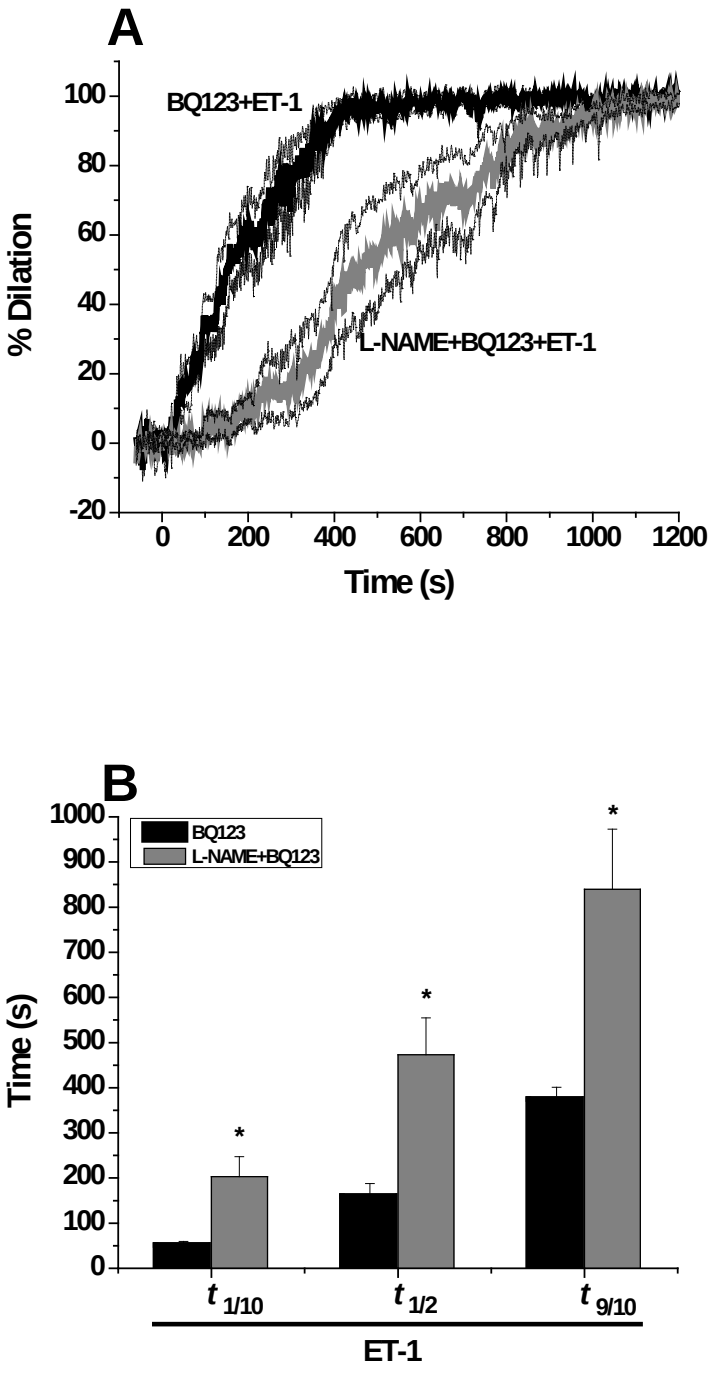
A
BQ123+ET-1
L-NAME+BQ123+ET-1
% Dilation
Time (s)
100
80
60
40
20
0
-20
0
200
400
600
800
1000
1200
B
BQ123
L-NAME+BQ123
Time (s)
1000
900
800
700
600
500
400
300
200
100
0
*
*
*
t 1/10
t 1/2
t 9/10
ET-1

Figure S6

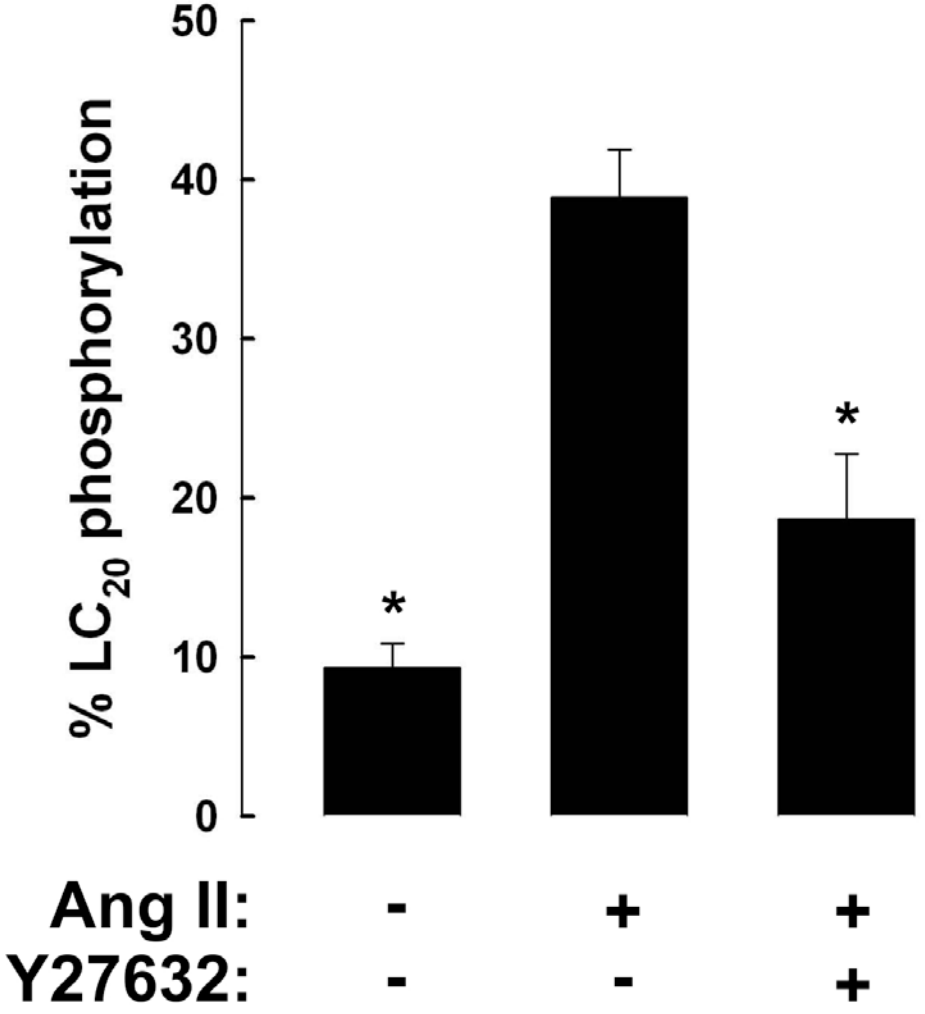

Figure 1

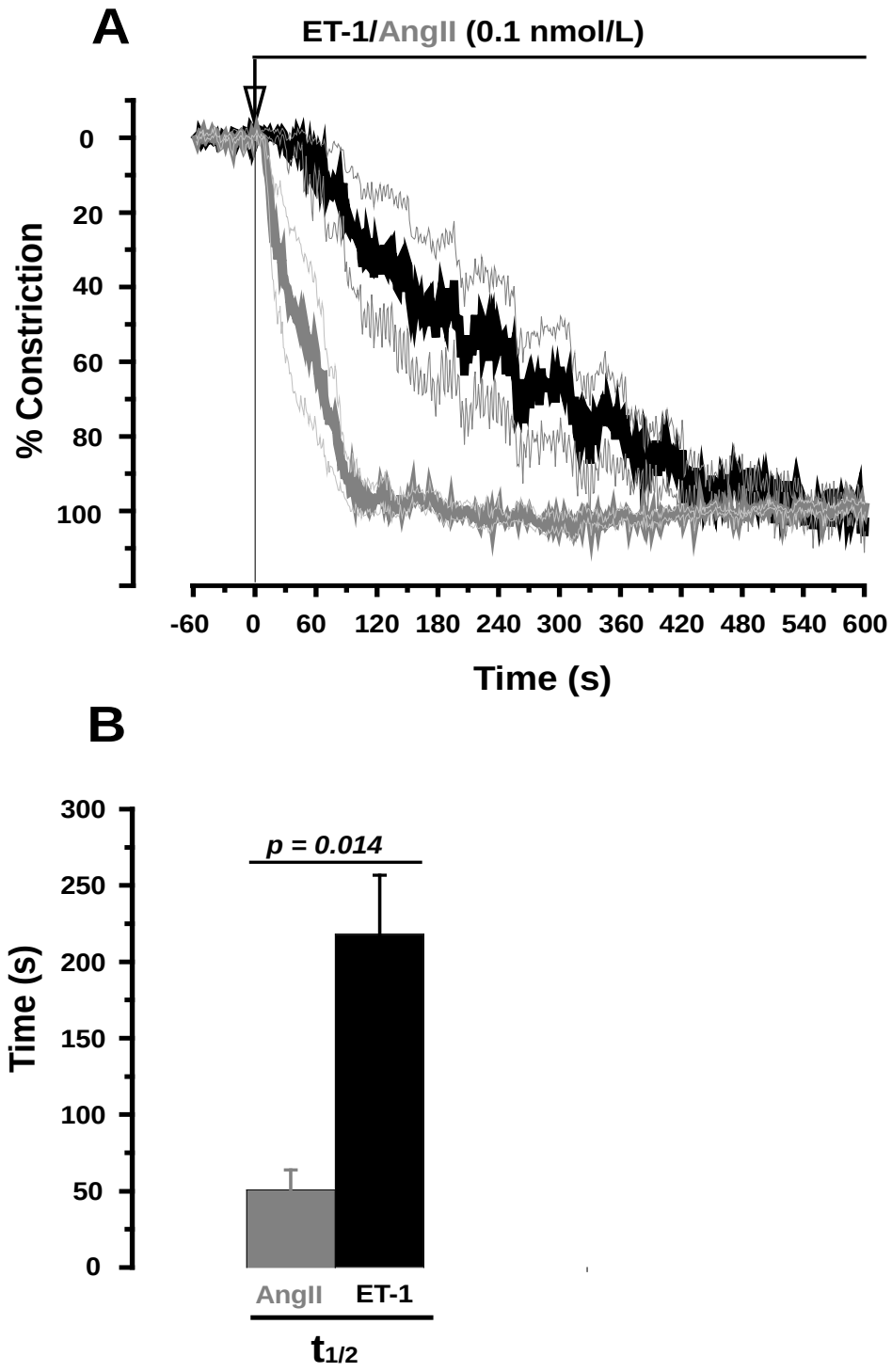
A
ET-1/AngII (0.1 nmol/L)
% Constriction
0
20
40
60
80
100
-60
0
60
120
180
240
300
360
420
480
540
600
Time (s)
B
Time (s)
300
250
200
150
100
50
0
p = 0.014
AngII
ET-1
t1/2

Figure 2

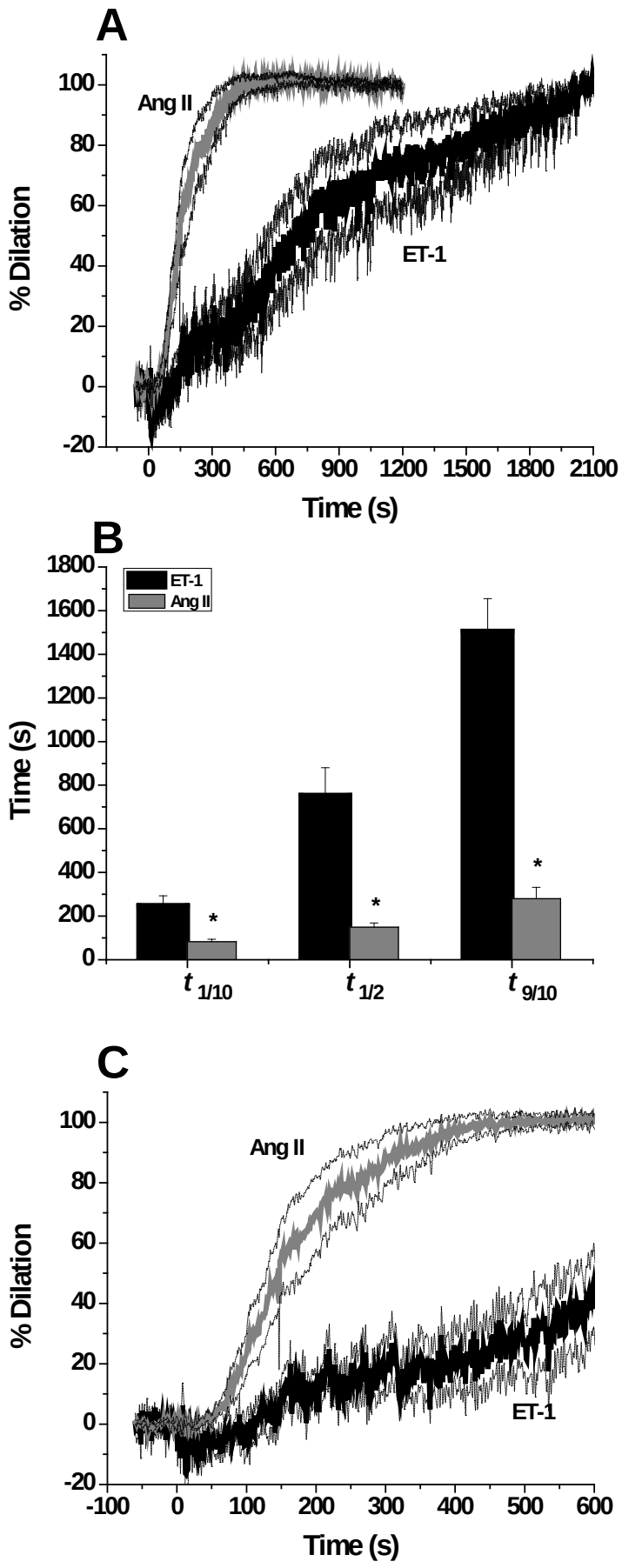
A
Ang II
ET-1
% Dilation
Time (s)
B
ET-1
Ang II
Time (s)
$t_{1/10}$
$t_{1/2}$
$t_{9/10}$
C
Ang II
ET-1
% Dilation
Time (s)

Figure 3

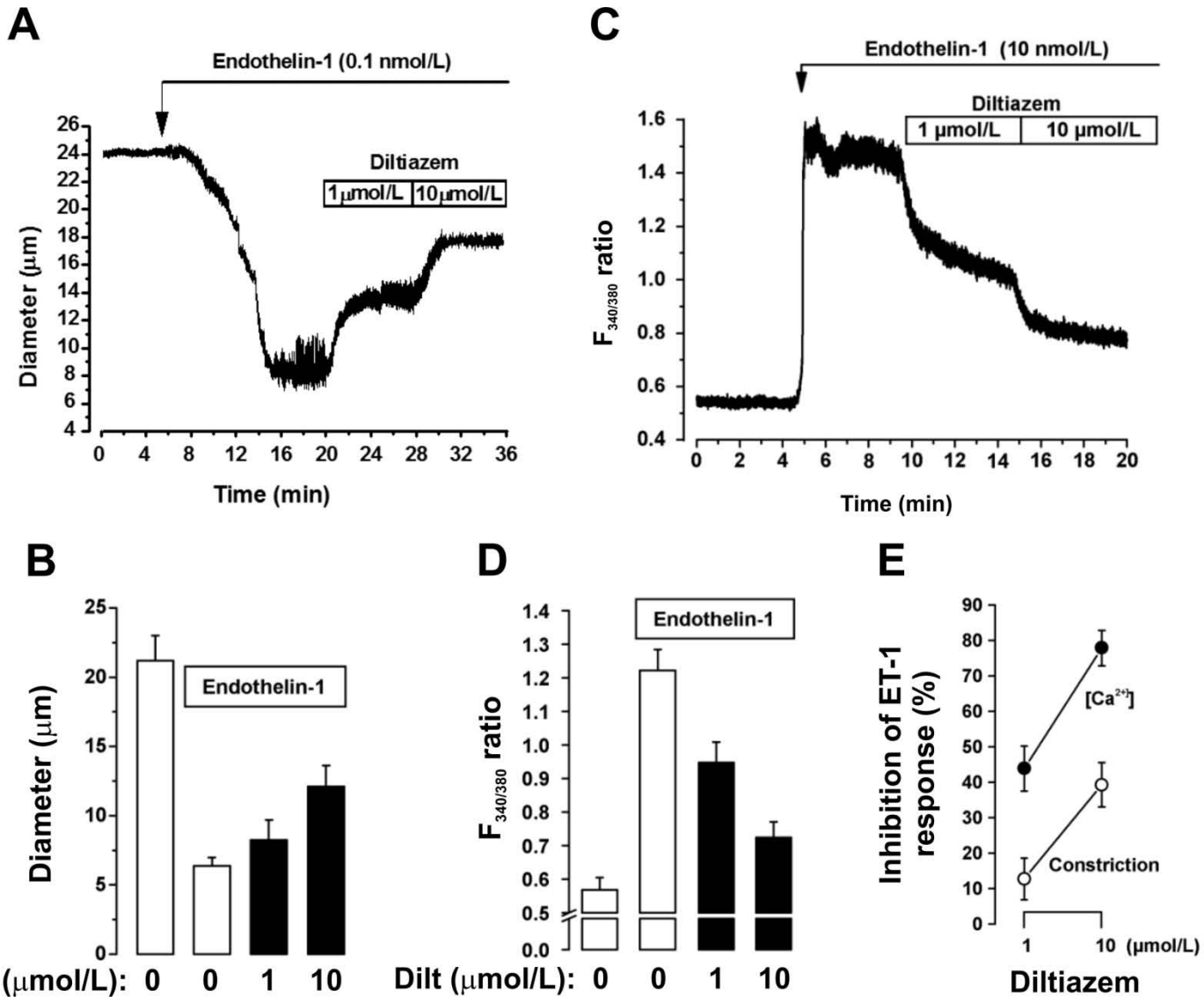
A
Endothelin-1 (0.1 nmol/L)
Diltiazem
1 μmol/L
10 μmol/L
Diameter (μm)
Time (min)
C
Endothelin-1 (10 nmol/L)
Diltiazem
1 μmol/L
10 μmol/L
F340/380 ratio
Time (min)
B
Endothelin-1
Diameter (μm)
Dilt (μmol/L): 0 0 1 10
D
Endothelin-1
F340/380 ratio
Dilt (μmol/L): 0 0 1 10
E
Inhibition of ET-1 response (%)
[Ca2+]
Constriction
1
10 (μmol/L)
Diltiazem

Figure 4

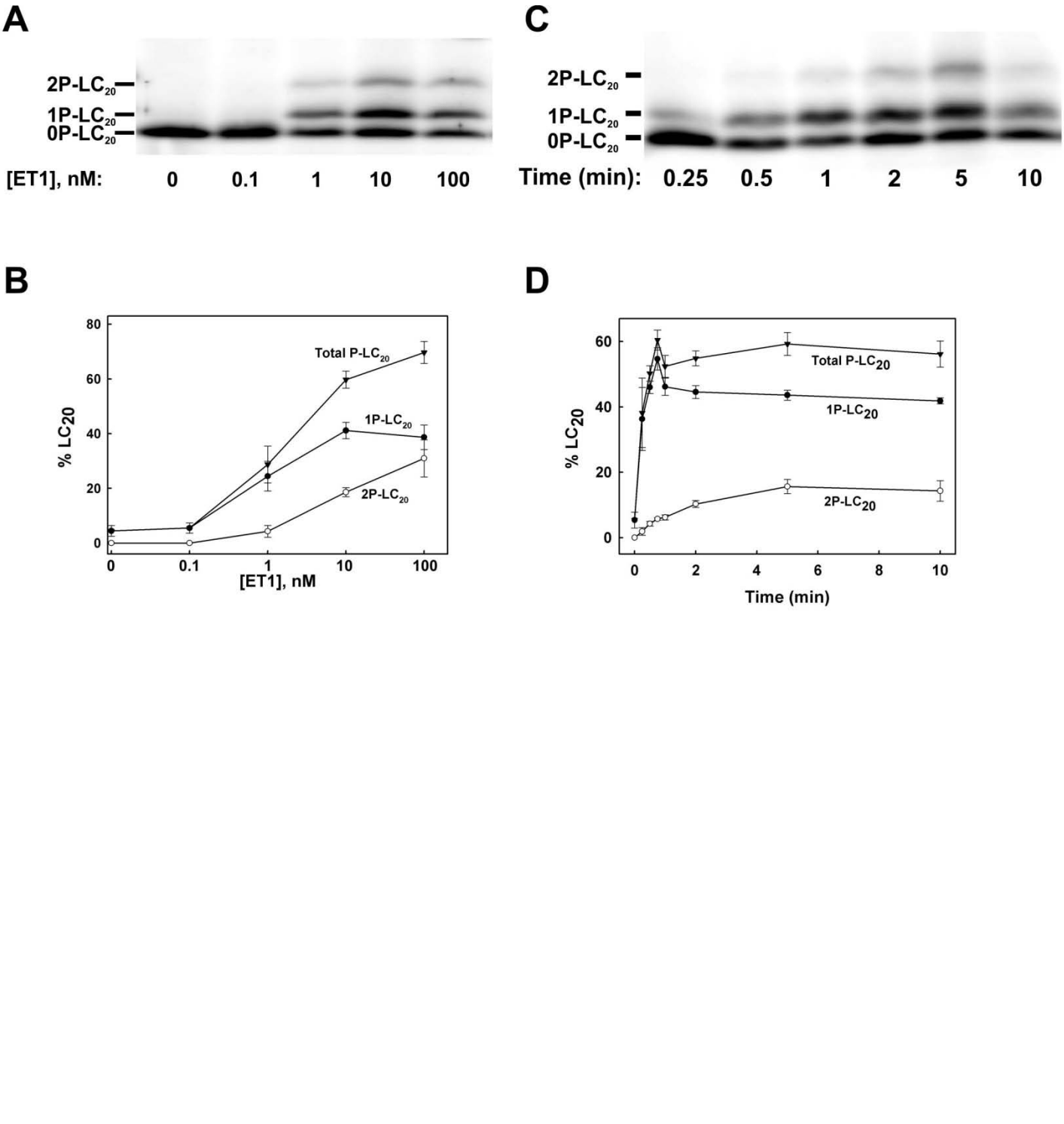
A
2P-LC20
1P-LC20
0P-LC20
[ET1], nM: 0 0.1 1 10 100
C
2P-LC20
1P-LC20
0P-LC20
Time (min): 0.25 0.5 1 2 5 10
B
% LC20
Total P-LC20
1P-LC20
2P-LC20
[ET1], nM
D
% LC20
Total P-LC20
1P-LC20
2P-LC20
Time (min)

Figure 5

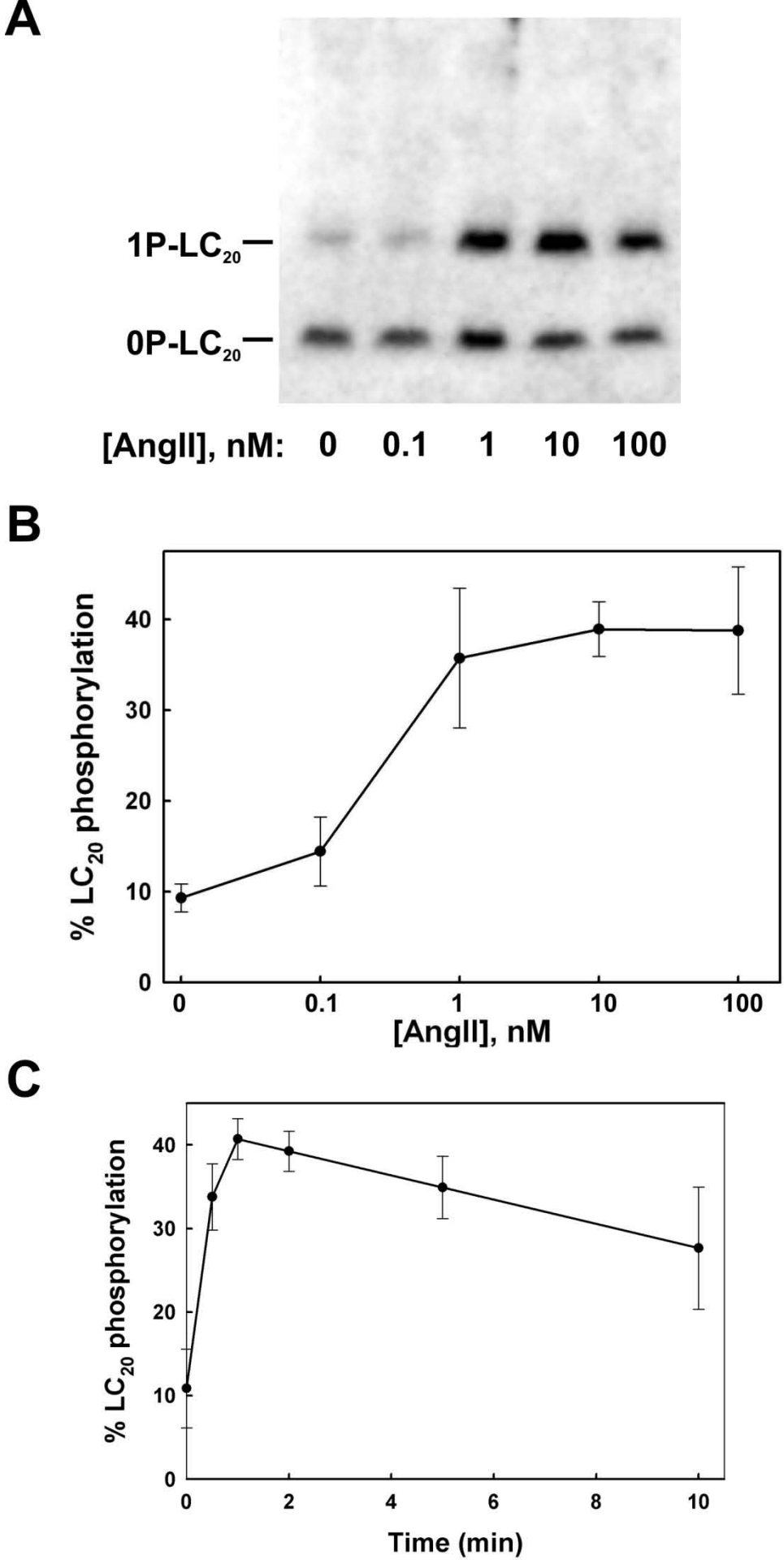
A
1P-LC20
0P-LC20
[AngII], nM: 0 0.1 1 10 100
B
% LC20 phosphorylation
0
10
20
30
40
0
0.1
1
10
100
[AngII], nM
C
% LC20 phosphorylation
0
10
20
30
40
0
2
4
6
8
10
Time (min)

Figure 6

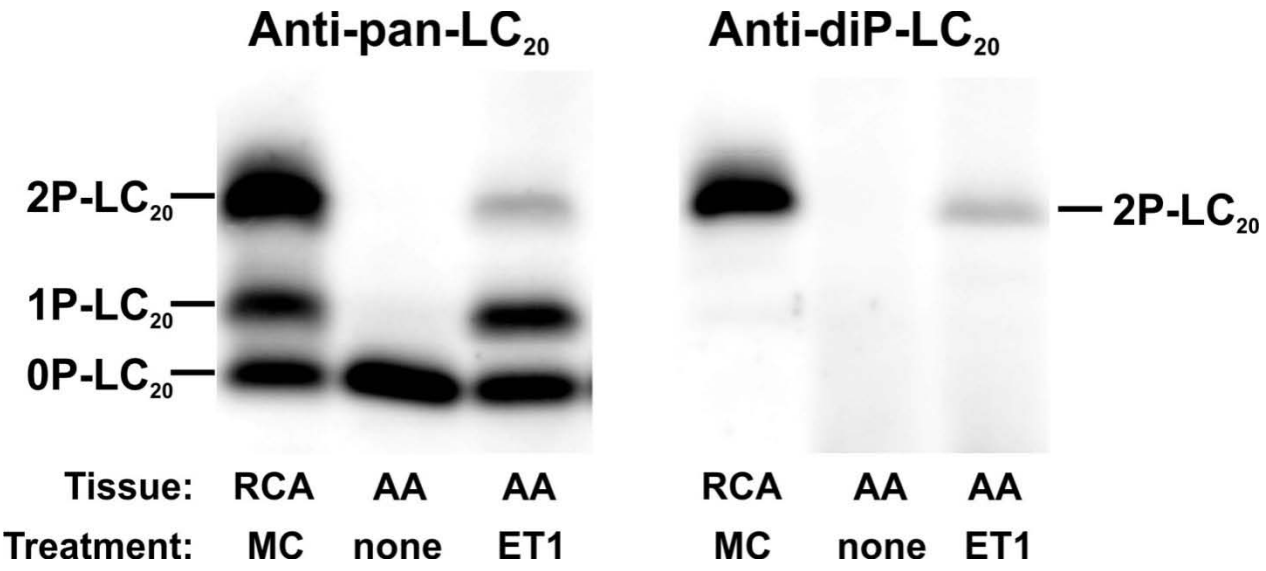
Anti-pan-LC20
Anti-diP-LC20
2P-LC20
1P-LC20
0P-LC20
2P-LC20
Tissue: RCA AA AA RCA AA AA
Treatment: MC none ET1 MC none ET1

Figure 7

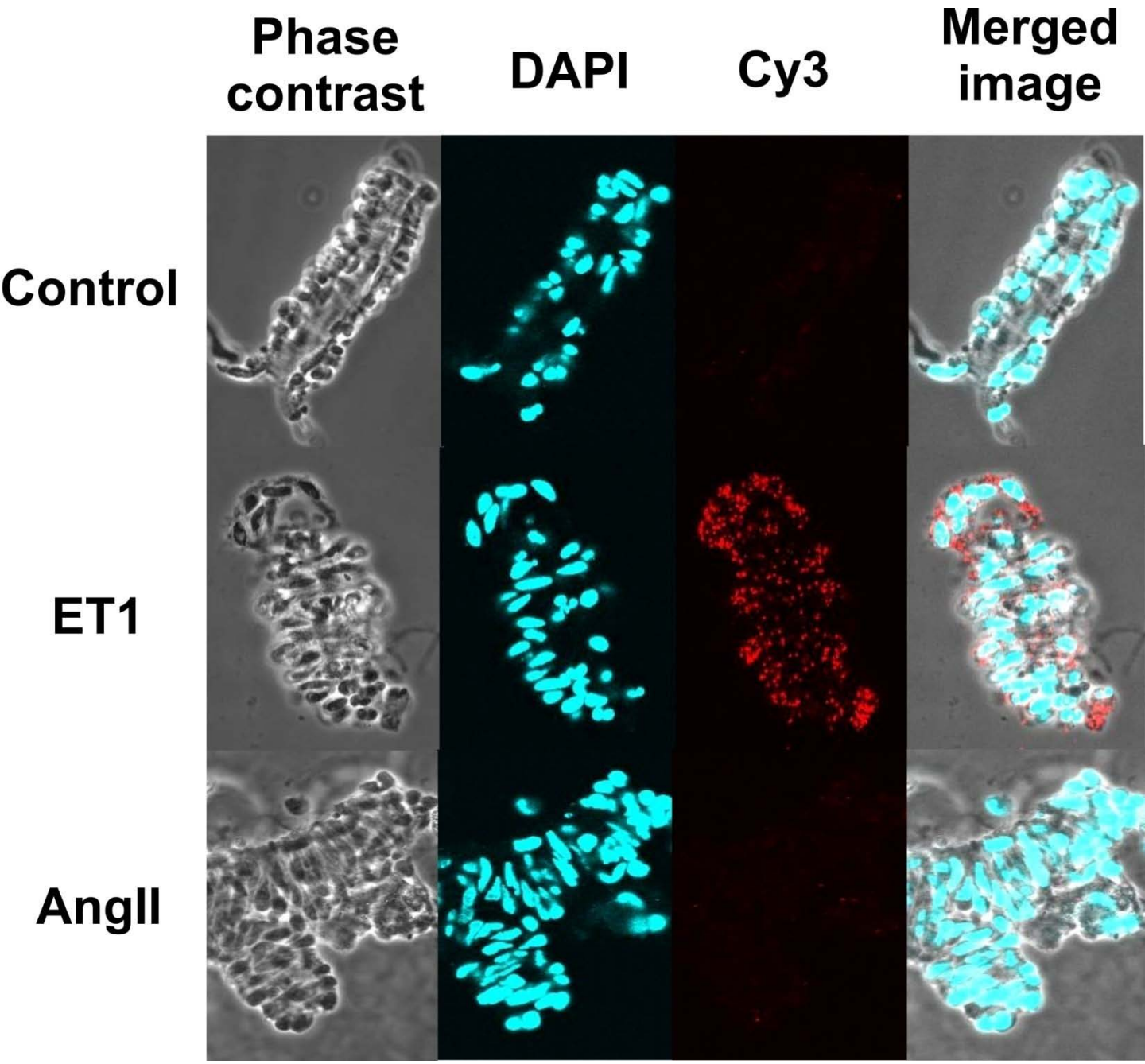

Figure 8

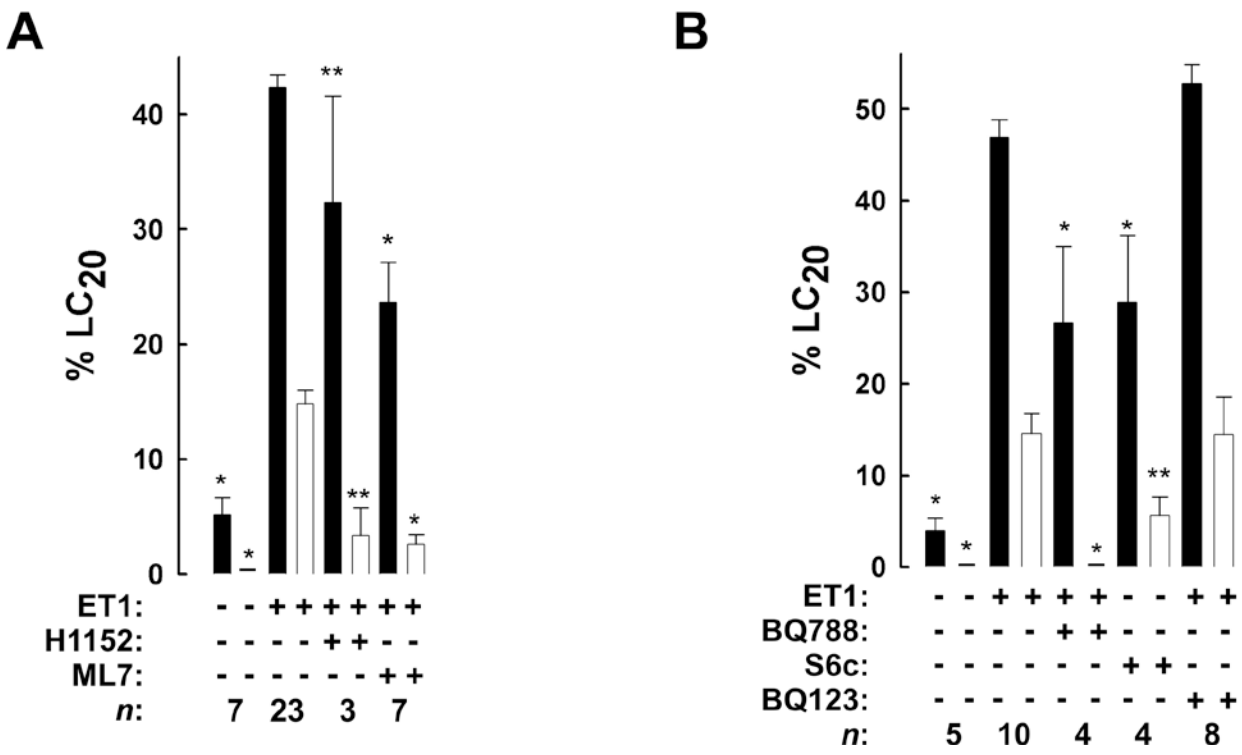
A
% LC20
0
10
20
30
40
*
*
**
**
*
*
ET1: - - + + + + + +
H1152: - - - - + + - -
ML7: - - - - - - + +
n: 7 23 3 7
B
% LC20
0
10
20
30
40
50
*
*
*
*
**
ET1: - - + + + + - - + +
BQ788: - - - - + + - - - -
S6c: - - - - - - + + - -
BQ123: - - - - - - - - + +
n: 5 10 4 4 8

Figure 9

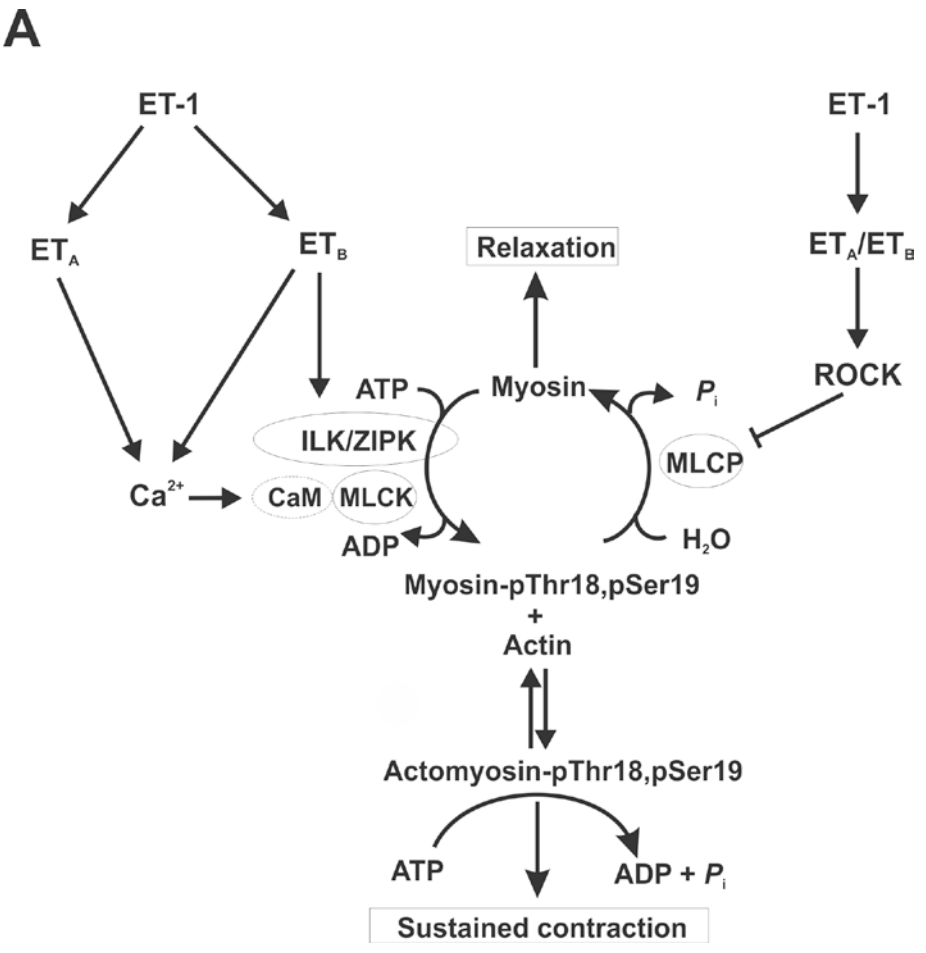
A
ET-1
ET-1
ET$_A$
ET$_B$
Relaxation
ET$_A$/ET$_B$
ROCK
ATP
Myosin
P_i
ILK/ZIPK
MLCP
Ca^{2+}
CaM
MLCK
ADP
H$_2$O
Myosin-pThr18,pSer19
+
Actin
Actomyosin-pThr18,pSer19
ATP
ADP + P_i
Sustained contraction
B
AngII
AngII
AT$_1$R
Relaxation
AT$_1$R
ROCK
ATP
Myosin
P_i
Ca^{2+}
CaM
MLCK
MLCP
ADP
H$_2$O
Myosin-pSer19
+
Actin
Actomyosin-pSer19
ATP
ADP + P_i
Contraction